CENTROSOME LOSS TRIGGERS A TRANSCRIPTIONAL PROGRAM TO COUNTER APOPTOSIS-INDUCED OXIDATIVE STRESS

John S Poulton [1,2,3] *, Daniel J McKay [1,4,5], and Mark Peifer [1,3] *

University of North Carolina at Chapel Hill

1. Department of Biology
2. Department of Medicine
3. Lineberger Comprehensive Cancer Center
4. Department of Genetics
5. Integrative Program for Biological and Genome Sciences

*Address correspondence to:

Mark Peifer: peifer@unc.edu

Or

John Poulton: poultonj@email.unc.edu

Abstract

Centrosomes play a critical role in mitotic spindle assembly through their role in microtubule nucleation and bipolar spindle assembly. Loss of centrosomes can impair the ability of some cells to properly conduct mitotic division, leading to chromosomal instability, cell stress, and aneuploidy. Multiple aspects of the cellular response to mitotic error associated with centrosome loss appears to involve activation of JNK signaling. To further characterize the transcriptional effects of centrosome loss, we compared gene expression profiles of wildtype and acentrosomal cells from Drosophila wing imaginal discs. We found elevation of expression of JNK target genes, which we verified at the protein level. Consistent with this, the upregulated gene set showed significant enrichment for the AP1 consensus DNA binding sequence. We also found significant elevation in expression of genes regulating redox balance. Based on those findings, we examined oxidative stress after centrosome loss, revealing that acentrosomal wing cells have significant increases in reactive oxygen species (ROS). We then performed a candidate genetic screen and found that one of the genes upregulated in acentrosomal cells, G6PD, plays an important role in buffering acentrosomal cells against increased ROS and helps protect those cells from cell death. Our data and other recent studies have revealed a complex network of signaling pathways, transcriptional programs, and cellular processes that epithelial cells use to respond to stressors like mitotic errors to help limit cell damage and maintain normal tissue development.

Introduction

Proper development requires precise spatial and temporal coordination of cell division to drive tissue growth. During cell division, chromosomes are replicated in S phase, and then segregated equally into two daughter cells during mitosis. The accurate segregation of chromosomes is achieved by the action of the bipolar mitotic spindle (WALCZAK AND HEALD 2008). This microtubule-based structure is essential to generate the physical forces required to move chromosomes to opposite poles, and also has built-in checkpoints that ensure accurate segregation. The assembly of the mitotic spindle is a complex process with multiple layers of regulation to ensure its accuracy (PROSSER AND PELLETIER 2017). Defects in mitotic spindle formation can lead to multipolar spindles or incorrect attachment of microtubules (MTs) to chromosomes, which in turn can lead to segregation errors that cause DNA damage and even whole chromosome mis-segregation (aneuploidy). These types of defects are forms of chromosomal instability (CIN), a hallmark of many cancers that is highly correlated with tumor malignancy (HANAHAN AND WEINBERG 2011; NICHOLSON AND CIMINI 2011).

In most animal cells, the bipolar mitotic spindle arises from the MT nucleating activity of a pair of organelles known as centrosomes, which sit at the two spindle poles (Figure 1A)(WALCZAK AND HEALD 2008; LERIT AND POULTON 2016; PROSSER AND PELLETIER 2017). As the central source of spindle MTs, the orientation of the centrosome pair also determines the geometry of mitotic spindle formation and the axis of division relative to the surrounding tissue. Thus, even within mitosis, centrosomes serve multiple functions related to spindle assembly. Centrosomes also serve a wide range of cellular functions separate from mitotic spindle assembly, including regulation of cilia assembly, cell cycle progression, the DNA damage response, and cell signaling. Given these critical functions ascribed to centrosomes, they were long considered essential components of most animal cells.

More recently, however, it has become apparent that cells possess centrosome-independent MT nucleation pathways that assist in spindle assembly (e.g., the Augmin complex and RanGTP pathway)(PROSSER AND PELLETIER 2017). In many cell types, these additional pathways are robust and capable of assembling a bipolar spindle even in the complete absence of centrosomes. A striking example of this occurs in Drosophila where

entire animals homozygous mutant for genes essential for centrosome formation or function can develop to adulthood (BASTO *et al.* 2006). We now know this is not unique to flies, because if p53-mediated program cell death is blocked, mice lacking centrosomes can develop to late embryogenesis and then die because the lack of cilia impairs Hedgehog signaling (BAZZI AND ANDERSON 2014).

In Drosophila, detailed examinations of acentrosomal cells in several tissues (e.g., brain and ovarian germline) revealed surprisingly few mitotic errors, indicating the non-centrosomal MT nucleation pathways are adequate for proper spindle assembly and accurate chromosome segregation in those cells (BASTO *et al.* 2006; STEVENS *et al.* 2007; POULTON *et al.* 2017). In contrast to studies in those tissues, we previously found that in the proliferative epithelial cells of the wing imaginal disc, loss of those same centrosomal proteins leads to significant defects in spindle assembly, which increases rates of aneuploidy, DNA damage, and mis-oriented spindles (POULTON *et al.* 2014). Those defects then activate a cell stress pathway, cJun N-terminal Kinase (JNK) signaling, which drives apoptotic cell death (Figure 1B-E). Approximately 15-20% of all cells in acentrosomal wing discs die, suggesting that although alternative MT nucleation pathways help buffer wing disc cells against centrosome loss, they are not as effective in this tissue as they appear to be in other tissues/cell types. Despite the loss of such a substantial fraction of cells, overall wing development remains remarkably normal in most centrosome-deficient animals. Proper mitosis and subsequent wing development in acentrosomal animals are mediated by a number of factors. Correct spindle assembly becomes dependent on MT nucleation by the Augmin complex and RanGTP pathway, and on delay of the cell cycle by the Spindle Assembly Checkpoint (SAC). The cell death that does occur is buffered by compensatory proliferation of neighboring cells to replace dying cells, and delayed development, which presumably allows additional time to correct tissue-level defects caused by massive cell death (POULTON *et al.* 2014). Together, those findings highlighted the remarkable ability of cells and tissues to compensate, not only for loss of key mitotic regulators, such as centrosomes, but also for the wide range of downstream effects of their loss, such as CIN and cell death.

The sensitivity of wing disc cells to mitotic spindle assembly errors due to centrosome loss, as well as their sensitivity to the downstream consequences of spindle

assembly errors (i.e., aneuploidy and spindle mis-orientation), make them an excellent model to investigate the cellular response to centrosome loss, mitotic errors, and cell death, as well as the tissue-level and systemic responses to those insults. As our previous data and others demonstrated, one important component of these complex responses to tissue damage induced by a variety of stresses are changes in gene expression, the most well-characterized of which are associated with activation of cell signaling pathways (i.e., JNK, Wnt, Dpp, and JAK-STAT)(RYOO *et al.* 2004; KONDO *et al.* 2006; PASTOR-PAREJA *et al.* 2008; PEREZ-GARIJO *et al.* 2009; DEKANTY *et al.* 2012; POULTON *et al.* 2014). For example, it is now clear that JNK signaling is a central mediator of the response to multiple forms of cell stress or tissue damage (IGAKI 2009). High levels of JNK activity initiates apoptosis in tissues like the wing and eye imaginal discs. To help compensate for the loss of cells due to apoptosis, lower levels of JNK in neighboring cells can help drive proliferation in the surviving cells to help maintain total cell numbers and tissue integrity, which is a central component of the regeneration process (RYOO *et al.* 2004; FAN AND BERGMANN 2008; MARTIN *et al.* 2009; PEREZ-GARIJO *et al.* 2009; FOGARTY *et al.* 2016; BROCK *et al.* 2017; KHAN *et al.* 2017). Several recent studies demonstrate the important transcriptional responses occurring in damaged/stressed cells, much of it mediated directly by JNK signaling. For example, one key pathway that helps drive the compensatory proliferation response is JAK-STAT signaling, whose activating ligands (the Unpaired (Upd) proteins) are themselves transcriptional targets of JNK signaling (PASTOR-PAREJA *et al.* 2008; BUNKER *et al.* 2015; SANTABARBARA-RUIZ *et al.* 2015). Intriguingly, recent studies also uncovered important effects of cell stress and damage on redox balance in imaginal discs, and suggest important roles for reactive oxygen species (ROS) in mediating the activity of the relevant cell signaling pathways to control processes like cell death and compensatory proliferation (KANDA *et al.* 2011; OHSAWA *et al.* 2012; GAURON *et al.* 2013; HUU *et al.* 2015; SANTABARBARA-RUIZ *et al.* 2015; CLEMENTE-RUIZ *et al.* 2016; FOGARTY *et al.* 2016; BROCK *et al.* 2017; KHAN *et al.* 2017; PEREZ *et al.* 2017). Together these studies have begun to elucidate a regulatory network involving complex cross-talk between traditional signaling pathways and ROS that helps correct for cellular damage and maintain tissue homeostasis.

We sought to define the transcriptional response to centrosome loss. To do so, we performed transcriptome analysis on imaginal wing discs from wild type (WT) animals, and from two centrosome-lacking genotypes. Differential gene expression analysis identified hundreds of genes that are significantly up or down-regulated in both acentrosomal mutants relative to WT. One key finding from the transcriptional data, and our subsequent functional genetics experiments, is that centrosome loss induces significant oxidative stress—many of the genes upregulated in acentrosomal cells contribute to redox regulation. We then performed a reverse genetic screen in the genetically sensitized background of acentrosomal wing disc cells and identified a novel genetic interaction between *sas-4*, which encodes a core centrosomal protein, and the gene encoding Glucose-6-phosphate dehydrogenase *(g6pd)*, the rate limiting enzyme in the pentose phosphate pathway and key generator of the antioxidant reduced Glutathione (STANTON 2012). We went on to characterize the cellular defects underlying this interaction, and found that G6PD upregulation is an important counter-balance to increased Reactive Oxygen Species (ROS) induced by mitotic errors. Together, the current study reveals new consequences of centrosome loss (i.e., oxidative stress/redox imbalance), as well as yet another way in which acentrosomal cells buffer themselves against the deleterious effects of centrosome loss (i.e., upregulation of antioxidant promoting genes to limit ROS levels).

Results

Defining the transcriptional response to centrosome loss

To investigate the effects of centrosome loss on the transcriptional program of a developing tissue, we performed RNA-Seq on *Drosophila* wing imaginal discs from late 3rd instar larvae of three genotypes: *yellow white* (*y w*; our wildtype (WT) control), or animals homozygous mutant for null alleles of one of two different proteins required for centriole duplication: *sas-4*^{s2214} or *asl*^{mecD}. Previous studies demonstrate that these alleles lead to complete or near-complete loss of centrosomes by 3rd larval instar (BASTO *et al.* 2006; BLACHON *et al.* 2008; POULTON *et al.* 2014). We performed RNA-Seq on three biological replicates for each genotype. We first analyzed how well the replicates within a genotype correlated with one another, finding extremely high concordance among replicates for each genotype (Figure 2A; Pearson correlation coefficient=0.99 for replicates within each

genotype). We then examined the expression of the *sas-4* and *asl* loci in their respective mutant backgrounds. In the *sas-4* mutant there was almost complete loss of *sas-4* RNA transcripts (Figure 1F). It is worth noting that the *sas-4*^{s2214} mutant did possess transcripts of ~200bp arising from the 5' end of the first exon. The *sas-4*^{s2214} allele is a P-element insertion in the first exon, previously mapped to chromosomal location 3R:2977450, which is precisely where the abrupt end of transcripts was observed in the *sas-4* mutant. The *asl*^{mecD} mutation is a point mutant (C1718T), leading to a premature stop codon at Q483. Consistent with a point mutant, full length transcripts were present in the *asl*^{mecD} mutant background, though overall levels were slightly reduced compared to controls (Figure 1G), which may reflect Nonsense Mediated Decay.

To define changes in gene expression associated with centrosome loss, we compared RNA-Seq data from each of the acentrosomal mutants to the WT control RNA-Seq data. Plots of differential gene expression revealed many up and down-regulated genes for each pairwise genotype comparison (Figure 2A; complete lists of gene expression data are found in Suppl. Table 1). To identify the genes most significantly up or down-regulated in each mutant relative to WT, we filtered the comprehensive list of genes to include only those genes that met a False Discovery Rate (FDR) of $p<0.001$, as well as a minimum expression threshold (FPKM ≥ 10) for at least one genotype. In the comparison of *sas-4* mutant wing discs to controls, use of these filters revealed 495 genes significantly upregulated and 272 genes downregulated in *sas-4* discs (Suppl. Table 2). In the comparison of *asl* mutant wing discs to controls, we found 493 upregulated genes and 575 downregulated (Suppl. Table 3).

Mutations in *sas-4* and *asl* result in centrosome loss through different mechanisms—Sas-4 is directly involved in centriole assembly (KOHLMAIER *et al.* 2009; SCHMIDT *et al.* 2009), whereas Asl regulates daughter centriole duplication licensing (BLACHON *et al.* 2008; NOVAK *et al.* 2014). Therefore, changes in gene expression unique to one mutant genotype might reflect the transcriptional response to centrosome-independent functions for that particular protein. To identify the common response to centrosome loss, we cross-referenced the lists of differentially-expressed genes to identify sets of genes that were significantly up or down-regulated in both acentrosomal mutants relative to WT. The two lists exhibited highly significant overlap (Figure 2C,C'): 221 genes

were significantly upregulated (Suppl. Table 4) and 154 genes were significantly downregulated (Suppl. Table 5) in both *sas-4* and *asl* wing discs, relative to control wing discs. This was much higher than expected by chance (hypergeometric mean test: $p<4.26^{e-201}$ for upregulated genes; $p<1.54^{e-91}$ for downregulated genes). This conservative approach should exclude any unforeseen changes in gene expression associated with a particular mutant or mutant background, thus isolating only genes specifically affected by loss of centrosomes. Of course, for some genes, lack of concordance may simply result from experimental variability. Similarly, changes in gene expression for a particular gene might have reached the significance threshold in one genotype, but been just below that threshold in the other, thus excluding it from the shared list of significantly up or downregulated genes common to both.

Several categories of genes, as defined by GO-Term analysis via DAVID (HUANG DA *et al.* 2009), were notable in the list of jointly upregulated genes. These included genes involved in oxidation-reduction pathways, including the antioxidant and detoxifying glutathione transferase pathway, as well as genes involved in the innate immune response (Tables 1-3). Manual inspection also revealed a number of genes involved in or known to be targets of the JNK pathway (Table 4), consistent with our previous work (POULTON *et al.* 2014).

The transcriptional response to centrosome loss does not broadly elevate core centrosomal proteins or proteins involved in parallel pathways

Centrosomes are multi-protein organelles. We thus had initially hypothesized that cells might sense the mitotic challenge in centrosome-deficient cells by upregulating the genes encoding centrosomal proteins. However, no known centrosomal components were on the list of genes significantly upregulated in both *asl* mutants and *sas-4* mutants. Centrosome loss in wing imaginal discs is buffered by the mitotic delay induced by the SAC and by the microtubule nucleation that mediates non-centrosomal spindle assembly. Thus another potential transcriptional response might be upregulation of the components of the SAC, Augmin complex, or Ran pathway, which partially compensate for centrosome loss in wing discs as well as in the early embryo (HAYWARD *et al.* 2014; POULTON *et al.* 2014). Only two genes with microtubule or SAC connections were on the list of genes significantly

upregulated by loss of both Asl and Sas-4: Tubulin binding cofactor A (CG1890)(VOELZMANN *et al.* 2016), and Spindly, a protein essential for silencing the SAC via dynein recruitment to the kinetochore (GRIFFIS *et al.* 2007). However, when we scanned the lists of genes upregulated by knockdown of *sas4* or *asl* alone, a few additional genes emerged: *rcd2,* identified in an RNAi screen for centrosome function (DOBBELAERE *et al.* 2008), and *CP309*, encoding the centrosomal protein Pericentrin-like protein (PLP)(MENNELLA *et al.* 2012; LERIT *et al.* 2015; RICHENS *et al.* 2015), were upregulated in *sas-4* mutants, while *mad2*, a key component of the spindle assembly checkpoint (MUSACCHIO 2015), *ran*, which has dual roles in nuclear import and in non-centrosomal microtubule nucleation (CLARKE AND ZHANG 2008), and *cct5*, involved in centrosome-independent spindle assembly (MOUTINHO-PEREIRA *et al.* 2013), were upregulated in *asl* mutants. Thus coordinated transcriptional upregulation of the compensatory pathways does not appear to be a prominent response to loss of centrosomes, but it may play a minor role.

Centrosome loss in the wing imaginal disc disrupts mitotic spindle assembly, leading to chromosome mis-segregation and DNA damage (POULTON *et al.* 2014). The DNA damage response (DDR) is a complex, multi-tiered process wherein damage to DNA initiates repair pathways to correct the lesions, or, if the damage is too severe, triggers programmed cell death (BORGES *et al.* 2008). One aspect of the DDR is upregulation of genes involved in DNA damage detection or repair (CHRISTMANN AND KAINA 2013). Interestingly, we did not detect significant up or downregulation of known DDR genes in our analysis. Among the many possible explanations for this are that the extent of DNA damage is not sufficient to detect by analysis of the entire tissue (DNA damage was only detected in a subset of cells in acentrosomal wing discs, possibly due to rapid elimination of damaged cells from the wing epithelium)(POULTON *et al.* 2014), or that changes in gene expression are not a primary component of the DDR in this tissue.

Validating differential gene expression associated with centrosome loss reveals significant upregulation of genes regulated by the JNK pathway

In wing discs lacking centrosomes (i.e., *sas-4* mutant), there are significant defects in efficient spindle assembly, accurate chromosome segregation, and proper spindle orientation, leading to increased apoptosis (Figure 1B,C)(POULTON *et al.* 2014). These

mitotic defects appear to drive apoptosis of affected cells by activation of JNK signaling, since blocking JNK signaling prevented apoptosis in acentrosomal wing discs (POULTON *et al.* 2014). JNK signaling regulates gene expression, at least in part through the key transcription factor AP-1, a heterodimer of Jun (Jun-related antigen (Jra) in flies) and Fos. Consistent with this, we previously found that a JNK signaling transcriptional reporter (TRE>GFP; expresses GFP under the control of a promoter containing Jun binding sites) is activated by centrosome loss (i.e., *sas-4* RNAi), both in cells undergoing apoptosis and also in other cells in the disc (Figure 1D,E)(POULTON *et al.* 2014). These data suggested that we would see elevated expression of JNK target genes in centrosome deficient discs, both at the transcript and protein levels.

We thus tested this hypothesis, focusing on the *sas-4* mutant because *sas-4* loss appeared to elicit a stronger transcriptional response than *asl* for many of the genes present on the shared list of differentially expressed genes. Many positively regulated transcriptional targets of JNK signaling have been identified in *Drosophila*. Consistently, mRNA levels of many of these, including *Jra* itself, *puckered* (*puc*), a feedback negative regulator of the JNK pathway, *Insulin-like peptide 8* (*Ilp8*), *Reaper* (*rpr*), *Matrix Metalloproteinase1* (*MMP1*), were elevated in both the *sas-4* and *asl* mutant backgrounds, relative to WT controls (Figure 3A,B,E,F,L,M; Suppl Table 4).

We next examined whether the changes in RNA transcript levels observed in RNA-Seq analysis led to changes in protein levels of JNK transcriptional-targets, by using antibodies to MMP1 and Jra. Control WT wing discs express little to no MMP1or Jra protein (Figure 3C,G; with the exception of peripodial cells, which express moderate levels of Jra). Consistent with the RNA-Seq data, we found that *sas-4* mutant discs had noticeable increases in both proteins (Figure 3D,H). Because Jra is an essential component of the JNK signaling pathway, we tested the importance of Jra expression in control and acentrosomal cells. While knocking down Jra or Sas-4 alone did not perturb wing development, knocking down both led to significant morphological defects (Figure 3I-K). This is consistent with our previous data demonstrating a role for JNK itself in maintaining tissue homeostasis in acentrosomal wing discs (POULTON *et al.* 2014). This interaction likely occurs through JNK's positive roles in apoptosis and/or compensatory proliferation stemming from centrosome loss.

Another interesting hit from our RNA-Seq screen was *Insulin-like peptide 8* (*Ilp8*)(Figure 3L,M; Suppl Table 4). Ilp8 mediates delays in developmental timing caused by abnormal tissue growth during larval stages (COLOMBANI *et al.* 2012; GARELLI *et al.* 2012). We found that larvae mutant for centrosomal proteins such as Sas-4 exhibit a significant delay in larval development, taking approximately 24hrs longer than controls to enter pupation (POULTON *et al.* 2014). We thus examined whether the increase in Ilp8 transcripts in centrosome-deficient animals leads to increased Ilp8 protein expression, using Ilp8:GFP, a GFP protein trap of the endogenous *Ilp8* locus (GARELLI *et al.* 2012). In control WT animals, there is minimal expression of Ilp8 in 3rd instar wing imaginal discs (Figure 3N). However, in *Ilp8:GFP sas-4* animals, we noted a significant increase in Ilp8:GFP expression (Figure 3O). Ilp8 upregulation in response to imaginal disc growth defects induced by knockdown of endocytic or ribosomal proteins (i.e., Avl or Rpl7) requires JNK signaling (COLOMBANI *et al.* 2012). We thus tested whether JNK signaling mediated the upregulation of Ilp8 after centrosome loss. Indeed, when we used the Gal4-UAS system to ectopically express a dominant negative form of the fly homologue of JNK (BasketDN; BskDN) in the posterior portion of *sas-4* homozygous mutant wing discs, this led to a clear reduction in Ilp8:GFP in the region of the disc where JNK was inhibited (Figure 3P). The increased Ilp8 expression in *sas-4* mutants, along with the known developmental delay and JNK activation experienced by these animals, suggests Ilp8 upregulation via JNK is likely an important mediator of prolonged development in acentrosomal animals.

These data demonstrate that, in the wing imaginal disc, centrosome loss leads to increased JNK activity with concomitant changes in expression of JNK target genes, and also validate the accuracy of our RNA-Seq data. It will be interesting to determine if some of the other genes differentially regulated by centrosome loss, as identified in our RNA-Seq data, are previously unknown JNK signaling targets—a growing number of transcriptomic studies from Drosophila models with active JNK signaling may provide valuable data for cross-referencing (ROUSSET *et al.* 2010; BUNKER *et al.* 2015; CLEMENTE-RUIZ *et al.* 2016; KHAN *et al.* 2017).

To examine this possibility in our own data, we performed transcription factor binding motif analysis of the shared genes upregulated in acentrosomal cells. We first

looked for enrichment of known transcription factor binding motifs in open chromatin sites of 3rd instar wing imaginal discs within 2kb of the 221 genes upregulated in both mutant backgrounds (=403 FAIRE peaks)(UYEHARA *et al.* 2017). Remarkably, a consensus sequence significantly matching the AP-1 binding site was found in 63 of the 403 FAIRE peaks (Figure 2D; $p=2.34^{e-8}$). This suggests that there may be many additional genes directly upregulated by JNK signaling in centrosome-deficient cells. To further test this possibility, we performed *de novo* motif discovery in those open chromatin regions within 2kb of the upregulated genes. This analysis revealed the presence of an AP-1 binding site in 121/403 FAIRE peaks (Figure 2E; $p=1.6^{e-6}$). Intriguingly, these analyses also revealed additional motifs unrelated to JNK signaling, including GAGA, GATA, and Lola binding sites (Figure 2D,E). Notably, GATA proteins, including the primary fly GATA protein Serpent, have recently been found to be regulated by ROS levels (GAO *et al.* 2014; INDO *et al.* 2017), and help promote the innate immune response (SENGER *et al.* 2006)—as noted above, centrosome loss increases expression of genes involved in oxidative stress and innate immune responses (Table 1). It will be interesting in the future to test possible roles for these transcription factors in the response to centrosome loss. It is also worth noting that neither *de novo* nor motif-enrichment analyses applied to genes downregulated in acentrosomal cells revealed any significant support for particular transcription factor binding sites near to those genes.

Based on the upregulation of the JAK-STAT ligands Upd2 and Upd3 in acentrosomal cells (Suppl. Table 4), it was curious that the STAT92E binding motif was not found in our *de novo* search (Figure 2E; the STAT92E consensus sequence was absent from the library of motifs used in our directed search). We therefore conducted a third analysis of potential transcription factor binding sites in the open chromatin around the genes up or downregulated in *sas-4* and *asl*, this time specifically looking for enrichment of sequences aligning to the STAT92E binding motif. In this analysis, we used the consensus AP-1 binding motif as a positive control since it was found to be significantly enriched in the upregulated genes based on both of our other motif search approaches (Figure 2D,E). This analysis revealed significant enrichment of STAT92E binding sites in the open chromatin regions of genes upregulated by centrosome loss (Figure 2F). In contrast, there was no significant enrichment of STAT92E binding sites in genes

downregulated by centrosome loss. To more directly determine whether *sas-4* knockdown leads to upregulation of JAK-STAT activity in acentrosomal cells, we examined expression of the JAK-STAT transcriptional reporter 10xSTAT:GFP in *sas-4* mutant wing discs. While, we did not detect obvious changes in JAK-STAT activity in *sas-4* mutants, when we blocked apoptosis with p35, we did find increased JAK-STAT activity (Suppl Figure 1), suggesting that centrosome loss leads to increased JAK-STAT activation, likely through JNK-induced upregulation of Upd ligands. Intriguingly, the strongest upregulation was in neighboring wildtype cells (Suppl Figure 1C, arrows), which may reflect JAK-STAT's involvement in the compensatory proliferation response.

Centrosome loss leads to oxidative stress

One of the most striking features of our RNA-Seq data was increased expression of a number of genes associated with the response to oxidative stress (Table 2). These ranged from signaling proteins like TNF-associated Factor 4 (TRAF4), which acts upstream of the JNK pathway to regulate the oxidative stress response (TANG *et al.* 2013), to enzymes like WW domain containing oxidoreductase (WWOX), which regulates ROS and TNF-induced cell death (O'KEEFE *et al.* 2015), or CG3714, a Nicotinate phosphoribosyltransferase family member that is essential for the increase in cellular NAD levels to prevent oxidative stress (HARA *et al.* 2007). Among these, multiple Glutathione S-transferase (GST) genes were upregulated in both *sas-4* and *asl* mutants, and *sas-4* loss led to upregulation of three additional GSTD genes (Figure 4A). These enzymes mitigate oxidative stress by conjugating glutathione to toxic electrophilic substrates, reducing their reactivity and increasing their solubility, thus facilitating their excretion from cells and tissues (CHATTERJEE AND GUPTA 2018).

We thus followed this lead, using GSTD1 as an example. GSTD1 is a known target of KEAP1/Nrf2 signaling, which regulates the response to oxidative stress (SYKIOTIS AND BOHMANN 2008). Experiments in the eye imaginal disc indicate GSTD1 can also be upregulated by JNK signaling (KANDA *et al.* 2011). Our RNA-seq data suggested that GSTD1 is upregulated in acentrosomal cells (Figure 4A-C). To confirm this, we took advantage of a GSTD1>GFP reporter, in which the promoter region of GSTD1 drives GFP expression (SYKIOTIS AND BOHMANN 2008). In WT discs, GSTD>GFP expression is very

low, while in *sas-4* mutant discs, there is strong upregulation of GFP driven by the GSTD1 promoter (Figure 4D,E). Interestingly, the consensus binding site for Nrf2 did not show up in our *de novo* transcription factor motif analysis (Figure 2E), nor was it found to be significantly enriched in our directed motif search of genes up or downregulated by centrosome loss (Figure 2F). Thus, despite significant upregulation of several oxidative stress response genes, including GSTD1, the number of direct targets of KEAP1/Nrf2 signaling in our upregulated gene set may be rather small.

Increased expression of GSTD genes, and in particular the upregulation of GSTD1>GFP, can reflect the presence of ROS (SYKIOTIS AND BOHMANN 2008). As noted above, Gene Ontology (GO) term analysis of our lists of genes significantly up or down-regulated in acentrosomal cells revealed changes in expression of proteins involved in both redox metabolism and detoxification associated with xenobiotic factors and oxidative stress. This could reflect an increase in reactive oxygen species (ROS) in cells lacking centrosomes. To test this hypothesis, we incubated *sas-4* mutant wing discs with the ROS probe dihydroethidium (DHE)(BINDOKAS *et al.* 1996). Strikingly, *sas-4* mutant wing discs had a dramatic increase in DHE staining (Figure 4F,G). We also observed increased signal using the MitoSOX probe, indicating at least some ROS production occurs in mitochondria (Figure 4H,I).

Centrosomes regulate several cellular processes that could conceivably affect redox balance (e.g., the DNA damage response)(LERIT AND POULTON 2016). We therefore sought to determine if the increase in ROS was a specific effect of centrosome loss, or a potential consequence of the mitotic errors induced by centrosome loss in the wing disc. Knockdown of key mitotic regulators and resulting mitotic errors were recently reported to lead to increased GSTD>GFP expression (CLEMENTE-RUIZ *et al.* 2016). We therefore used our ROS assays to examine ROS levels following knockdown of two other mitotic regulators, Mud and Bub3. Mud is important for spindle orientation in the wing disc (NAKAJIMA *et al.* 2013), while Bub3 contributes to the Spindle Assembly Checkpoint and the attachment of MTs to kinetochores (LOGARINHO *et al.* 2008). Thus, defects caused by knockdown of these proteins should be independent of centrosome function. As previously reported (DEKANTY *et al.* 2012; MORAIS DA SILVA *et al.* 2013; POULTON *et al.* 2014), knockdown of each of these proteins leads to significant increases in apoptosis (Figure 5A,C). We

found that Mud or Bub3 knockdown also increased ROS levels as measured by DHE staining (Figure 5B,D), similar to that observed after disruption of centrosome function. Together, these data are consistent with the possibility that ROS production increases in acentrosomal cells as a direct or indirect result of subsequent mitotic errors.

Recent studies in the wing disc suggest that apoptosis can induce ROS production, though this effect may be indirect (see Discussion)(SANTABARBARA-RUIZ *et al.* 2015; CLEMENTE-RUIZ *et al.* 2016; FOGARTY *et al.* 2016). To test the hypothesis that ROS induction we observed in centrosome deficient discs is a result of the apoptosis triggered by mitotic errors, we blocked apoptosis in *sas-4* homozygous mutant wing discs using the caspase inhibitor p35, and measured ROS levels. Blocking apoptosis significantly reduced ROS levels in *sas-4* mutant cells (Figure 5E,F,I). p35 blocks apoptosis by inhibiting the activity of the downstream caspase DrICE. However, it does not block activity of the upstream caspase Dronc, and this promotes continuous JNK activity in the resulting undead cells (KONDO *et al.* 2006; MARTIN *et al.* 2009). Thus the ability of p35 to block ROS elevation in *sas-4* mutant cells suggests that JNK activation alone is not sufficient to elevate ROS. (PEREZ *et al.* 2017)

The relationship between JNK signaling, apoptosis and ROS is complex. Activating JNK signaling can activate antioxidant pathways, and can also induce cell death (WANG *et al.* 2003; DHANASEKARAN AND REDDY 2017). We thus tested an alternate hypothesis: JNK signaling, while not sufficient, is necessary for the elevation of ROS we observe in centrosome deficient wing discs. To test this, we examined *sas-4* homozygous mutant wing discs in which JNK signaling was blocked through misexpression of bskDN. As we have shown previously, JNK inhibition via BSK-DN expression suppresses virtually all the apoptosis normally caused by centrosome loss (Figure 5G)(POULTON *et al.* 2014). DHE staining in these discs revealed a significant reduction in ROS levels after JNK blockade (Figure 5H,I), consistent with the idea that JNK signaling is necessary for elevated ROS production in centrosome-deficient wing discs. Together, these data suggest that the increased ROS levels in *sas-4* mutant cells depend on the completion of apoptosis, regardless of whether JNK is hyperactivated (as in the p35+ cells) or blocked (as in the bskDN cells). These results are considered further in the Discussion.

G6PD expression buffers ROS production and G6PD knockdown elevates apoptosis caused by centrosome loss

Our earlier work revealed that mitotic errors induced by the absence of centrosomes trigger apoptosis in the aneuploid cells (POULTON *et al.* 2014). However, these data also revealed that many cells that are challenged with centrosome loss evade death, though their cell cycle is lengthened. One possibility is that some of genes upregulated in *sas-4* mutant wing cells help centrosome-deficient cells survive in the presence of mitotic stress. To test this hypothesis, we performed a small candidate RNAi screen testing for genetic interactions with *sas-4*, predicting that knockdown of genes encoding proteins that helped cells cope with centrosome loss would enhance the *sas-4* knockdown phenotype. The candidate genes were chosen based on their roles as key players in redox balance or related signaling pathways (Table 5). From this screen, we identified a significant interaction between *sas-4* and *Glucose-6-phosphate dehydrogenase (G6PD).* While knockdown of either gene alone had minimal effects on adult wing blade morphology, knocking down both genes led to a significant increase in wing blistering (Figure 6A,B)—the *g6pd* RNAi line was previously shown to significantly reduce G6PD levels and activity (TEESALU *et al.* 2017). G6PD is the rate-limiting enzyme in the pentose phosphate pathway, converting Glucose-6-phosphate to 6-phosphoglucono-s-lactone. This reaction also generates NADPH, which is used by Glutathione reductase to produce reduced Glutathione (GSH), a potent antioxidant. Thus, in many cell types, G6PD can be a central player in the ability to limit ROS levels (STANTON 2012).

In our previous analysis of other *sas-4* genetic interactions (POULTON *et al.* 2014), an increased adult wing blistering phenotype correlated with increased levels of apoptosis during larval stages. We therefore examined apoptosis levels, using activated Caspase staining, to determine if there is any enhancement or suppression of the *sas-4* apoptotic phenotype after knockdown of G6PD. While *g6pd* RNAi alone led to no detectable increase in apoptosis (Figure 6D vs F, quantified in C), apoptosis was significantly increased when *g6pd* was knocked down in acentrosomal cells relative to that observed in acentrosomal cells alone (Figure 6E vs G, quantified in C). This was consistent with the hypothesis that G6PD buffers the elevated ROS production induced by centrosome loss. To directly test this, we stained for DHE in *g6pd* knockdown cells in the *sas-4* mutant

background. Consistent with the hypothesis, we observed an even greater increase in ROS levels in acentrosomal cells that also lack G6PD (Figure 7B vs D, quantified in G), while G6PD knockdown alone did not elevate ROS (Figure 7C,G). These data suggest that elevated G6PD expression in centrosome-deficient cells helps prevent the death of some of the cells attempting to cope with the loss of centrosomes, presumably by limiting the amount of ROS.

These observations indicated that the increased expression of G6PD we observed in *sas-4* mutant cells, as revealed by our RNA-Seq data, might serve as a feedback response to limit apoptosis and ROS production. To test this, we overexpressed G6PD in *sas-4* mutants. Consistent with the role of G6PD in antioxidant generation, ROS levels were significantly reduced in the *sas-4* mutant cells overexpressing G6PD (Figure 7F vs B,G). Interestingly, overexpression of G6PD did not detectably affect the levels of apoptosis caused by centrosome loss (Figure 6E vs I, quantified in C). Together, these data indicate that the upregulation of G6PD is important in limiting ROS production, and reveal that although its basal level of expression helps prevent apoptosis in mitotically stressed acentrosomal cells that have not already entered the apoptotic path, increasing G6PD levels alone is not sufficient to eliminate apoptosis caused by centrosome loss (Figure 6I,C). This interpretation fits well with our observations above indicating that increased ROS levels are largely downstream of apoptosis, thus decreasing ROS in cells already firmly committed to the path to apoptosis would not necessarily be expected to decrease apoptosis in this context.

Discussion

Transcriptional responses to cellular and tissue injury are major determinants of cell behavior and homeostasis. Drosophila imaginal discs have served as powerful models to identify the primary signaling pathways and biological processes governing these responses, and to dissect their relationships to one another (BEIRA AND PARO 2016). JNK signaling is now well-established as a central player in these events. JNK serves multiple roles, including sensing the initiating cell stress, activating pathways that can alleviate cellular stress (e.g. DNA repair pathways)(HAYAKAWA *et al.* 2004; PICCO AND PAGES 2013), triggering apoptosis when damage is severe (IGAKI 2009), and promoting activation

of secondary, mitogenic signaling pathways through upregulation of their ligands, which ultimately drives large-scale processes of tissue repair such as compensatory proliferation (RYOO *et al.* 2004). More recently, in the context of cell/tissue damage, JNK has also been implicated in regulating redox balance (CLEMENTE-RUIZ *et al.* 2016; FOGARTY *et al.* 2016; KHAN *et al.* 2017), which appears to be an important aspect of the cellular and tissue-level response to that damage.

We are interested in the response to centrosome loss, and in the pathways that buffer and compensate for the mitotic defects and resultant apoptosis that centrosome loss causes in some tissues (POULTON *et al.* 2014; POULTON *et al.* 2017). To extend this analysis, we examined the transcriptional response to centrosome loss. This revealed that mitotic errors induced by centrosome loss trigger a complex transcriptional response in wing imaginal discs, including JNK-dependent changes in gene expression. Interestingly, a previous microarray-based study of transcriptome profiles in acentrosomal fly cells did not detect major changes in gene expression of multiple components of particular cellular processes (e.g., no upregulation of JNK or redox pathways)(BAUMBACH *et al.* 2012). We believe the most likely reason for this difference was that that study pooled RNA from larval wing discs and brains. As we and others have shown, larval fly brains are quite robust to centrosome loss and therefore do not noticeably activate cell stress responses, like JNK signaling (BASTO *et al.* 2006; POULTON *et al.* 2017). Thus, it is likely that the changes in gene expression occurring in acentrosomal wing discs were diluted out by the inclusion of RNA from the brains in those experiments. It is also possible that technological differences between RNA-Seq and microarray platforms also contributed to our ability to detect expression changes in numerous genes.

In our RNA-Seq analysis, multiple regulators of redox balance were significantly upregulated. This finding spurred us to investigate the oxidative stress levels of acentrosomal cells, revealing that a significant fraction of these cells have high levels of ROS. We went on to identify the upregulation of G6PD as an important component of the ability of acentrosomal cells to buffer themselves against oxidative stress. Together, our data demonstrate that error-prone, acentrosomal mitosis activates JNK signaling, leading to both induction of apoptosis and to increased ROS production (Figure 7H). Our data also revealed an important mechanism to deal with this threat—transcriptional changes in redox

regulators, including G6PD, which then can feedback into the process, limiting the extent of both ROS production and cell death, and thus potentially giving cells more time to fix mitotic errors without losing the affected cells.

ROS, JNK, apoptosis, and proliferation/repair: a complex network

Recent studies have begun to reveal the complexities of the signaling network linking ROS, JNK, apoptosis, and proliferation/repair, casting doubt on the idea that they form a simple linear pathway, and instead suggesting that the responses may vary depending on the tissue and damaging agent. It is well-established that high levels of JNK signaling can induce apoptosis in imaginal discs (IGAKI 2009). In imaginal discs, ROS production increases rapidly following cell stresses such as aneuploidy (CLEMENTE-RUIZ *et al.* 2016), and is also elevated following the initiation of the apoptotic pathway, whether it be triggered by genetic manipulations (i.e. misexpression of proapoptotic Hid or Rpr (SANTABARBARA-RUIZ *et al.* 2015; FOGARTY *et al.* 2016; BROCK *et al.* 2017; KHAN *et al.* 2017), in tumor-forming genetic models (OHSAWA *et al.* 2012; PEREZ *et al.* 2017), or by physical tissue damage (SANTABARBARA-RUIZ *et al.* 2015). However, trying to fit all the data into a single, simple linear pathway is difficult. Directly inducing apoptosis or triggering caspase activity without death can lead to ROS elevation (HUU *et al.* 2015; SANTABARBARA-RUIZ *et al.* 2015; FOGARTY *et al.* 2016; KHAN *et al.* 2017; PEREZ *et al.* 2017) but it is also well-established that elevating ROS can trigger apoptosis (CAMHI *et al.* 1995; MARTINDALE AND HOLBROOK 2002; REDZA-DUTORDOIR AND AVERILL-BATES 2016), and reducing ROS can limit the apoptotic response (O'KEEFE *et al.* 2015; CLEMENTE-RUIZ *et al.* 2016; FOGARTY *et al.* 2016). There is evidence that ROS production is induced by JNK-signaling (KHAN *et al.* 2017; PEREZ *et al.* 2017), but also evidence that ROS plays a role in activating JNK (WANG *et al.* 2003; OHSAWA *et al.* 2012; SANTABARBARA-RUIZ *et al.* 2015; CLEMENTE-RUIZ *et al.* 2016; FOGARTY *et al.* 2016; KHAN *et al.* 2017; PEREZ *et al.* 2017), and that JNK signaling can induce an antioxidant response (WANG *et al.* 2003). Finally, in some situations elevating ROS appears to reduce JNK signaling (BROCK *et al.* 2017).

The studies most relevant to our work are from the Milan lab, who examined the consequences of aneuploidy induced by disrupting the spindle assembly checkpoint or spindle assembly in eye and wing disc epithelia. The parallels with centrosome loss are

striking. As with centrosome loss (POULTON *et al.* 2014), disrupting spindle assembly by reducing levels of mitotic regulators such as Rod or Bub3 elevated incidence of mitotic defects like lagging chromosomes and elevated DNA damage, and the resulting aneuploid cells are removed by apoptosis (DEKANTY *et al.* 2012; CLEMENTE-RUIZ *et al.* 2016). However, if apoptosis is blocked, highly aneuploid cells accumulate and a JNK-dependent transcriptional response is triggered. The "undead cells" elevate expression of the morphogen Wingless and drive tissue overgrowth, paralleling the effects of centrosome loss (POULTON *et al.* 2014). In a follow-up study, two more parallels were identified (CLEMENTE-RUIZ *et al.* 2016). First, dying cells accumulate elevated levels of ROS, as measured by GSTD1-GFP. Second, they also induce a transcriptional response that includes a series of JNK target genes and a set of genes involved in buffering ROS.

In other cases, the apoptosis-JNK-ROS connections are even more complex. For example, in eye imaginal discs, when apoptosis is induced by expression of Hid but death is blocked by p35 expression, the production and release of extracellular ROS is triggered (FOGARTY *et al.* 2016). This leads to recruitment of hemocytes that secrete the TNFα relative Eiger, which in turn activates lower and thus non-apoptotic levels of JNK activation in neighboring cells (FOGARTY *et al.* 2016). This promotes expression of mitogenic signals that contribute to processes such as compensatory proliferation/regeneration and apoptosis-induced proliferation. The generation of extracellular ROS appears to rely on plasma membrane targeted ROS generators such as Dual Oxidase (DUOX)(FOGARTY *et al.* 2016; KHAN *et al.* 2017). Intriguingly, the DUOX maturation factor NIP, encoded by *moladietz (mol)*, is itself upregulated by JNK activity (KHAN *et al.* 2017). JNK-induced extracellular ROS (produced by the NIP-DUOX mechanism) then helps maintain JNK activity in neighboring cells to drive tissue repair (KHAN *et al.* 2017).

Comparing our findings with these and other studies reveals interesting similarities and differences. First, consistent with these studies, we find that induction of apoptosis caused by loss of centrosomes or other mitotic regulators can trigger ROS production. However, our p35 data suggest that completion of apoptosis is important for ROS production in acentrosomal cells, which contrasts with data indicating that blocking apoptosis did not reduce ROS levels associated with misexpression of Hid (FOGARTY *et al.*

2016) or CIN induction (CLEMENTE-RUIZ *et al.* 2016). This difference suggests that the circuitry of these interconnected processes may be wired differently in acentrosomal cells, leading to different experimental outcomes. For example, different tissues might have different responses downstream of Dronc, which remains active after p35-mediated apoptosis blockade. Further studies will be also required to elucidate the cellular mechanisms generating ROS in these systems; NIP-DUOX is an interesting candidate (see below).

It is also worth considering what our data suggest about the relationship between JNK activity and ROS levels. As described above, recent data indicate that JNK can drive ROS production through NIP-DUOX (KHAN *et al.* 2017). However, others found that JNK is not essential for ROS production in the wing disc in response to aneuploidy (CLEMENTE-RUIZ *et al.* 2016) and that JNK activation is not sufficient for ROS elevation in the eye disc (FOGARTY *et al.* 2016). In contrast, we found that blocking JNK signaling in acentrosomal cells reduced ROS levels, which is very similar to recent findings from the Bergmann lab, who found that blocking JNK in *scrib ras*^{v12} clones prevents ROS production (PEREZ *et al.* 2017). In our experiments, we speculate that the reduction in ROS levels after JNK blockade is due to the subsequent inhibition of apoptosis, because when we blocked acentrosomal cell death via p35 misexpression, which leads to hyperactive JNK signaling, we did not detect increased ROS levels, instead finding decreased ROS in the p35+ cells. Perhaps the sustained, high levels of JNK signaling in these undead cells somehow subverts the NIP-DUOX mechanism of ROS production, either directly or indirectly through massive upregulation of ROS antagonists, like G6PD. Alternately, the mechanism driving NIP-DUOX mediated ROS levels may not be active in acentrosomal cells. Indeed, despite clearly identifying the upregulation of numerous JNK targets, our RNA-Seq data did not detect any significant upregulation of *mol*, even in individual mutant gene lists (i.e., *sas-4* vs control or *asl* vs control). Thus it is possible that ROS production caused by centrosome loss occurs independently of NIP-DUOX. Of course, it is also plausible that differential sensitivities associated with different RNA-Seq protocols or downstream analyses may explain the absence of *mol* upregulation in our data. Thus, our data and others clearly suggest important links between cellular damage, JNK activation, initiation of the apoptotic cascade, and ROS production. However, the circuitry connecting these events and the

mechanisms underlying those relationships appears to vary depending on the nature or severity of the damage. This would benefit from further exploration.

JAK-STAT and KEAP1-Nrf2 signaling

Another signaling pathway implicated by our RNA-Seq data was the JAK-STAT pathway. In our list of upregulated genes shared by both *sas-4* and *asl*, we noted increased expression of Upd2 and Upd3, both ligands of the pathway and previously identified JNK targets (PASTOR-PAREJA *et al.* 2008; BUNKER *et al.* 2015; SANTABARBARA-RUIZ *et al.* 2015). This list also included inositol pentakisphosphate 2-kinase (Ipk1), which can regulate Jak-Stat signaling (SEEDS *et al.* 2015), and the JAK-STAT target gene *vir1* (DOSTERT *et al.* 2005). Indeed, we did detect enrichment of STAT92E binding sites in our set of genes upregulated in both *sas-4* and *asl* loss (Figure 2F), and saw upregulation of a JAK-STAT reporter in acentrosomal cells, though only when apoptosis is inhibited (Suppl Figure 1A-C). We attempted to test for genetic interactions by inducing simultaneous *upd2* and *sas-4* knockdown, but the severe phenotypes (massive apoptosis and abnormal adult wings) caused by knockdown of Upd2 alone precluded analysis of the interaction. Other studies demonstrate a role for JAK-STAT in regulating the compensatory proliferation and regeneration processes in damaged imaginal discs (OHSAWA *et al.* 2012; KATSUYAMA *et al.* 2015; SANTABARBARA-RUIZ *et al.* 2015; CLEMENTE-RUIZ *et al.* 2016). We speculate that the increased levels of JAK-STAT ligands we detected are likely involved in the compensatory proliferation response we previously demonstrated occurs in acentrosomal wing discs (POULTON *et al.* 2014).

We also looked for connections with the KEAP1-Nrf2 pathway, which is well known as an important regulator of cytoprotective responses to oxidative stress (SYKIOTIS AND BOHMANN 2008; LOBODA *et al.* 2016; SIES *et al.* 2017). Nrf2 is a bZIP transcription factor that positively regulates antioxidant response proteins. KEAP1 keeps it inactive by anchoring it in the cytoplasm and targeting it for proteasomal destruction, but oxidative stress relieves this inhibition (Figure 7H). G6PD is a target of KEAP1-Nrf2 signaling (LOBODA *et al.* 2016). Many of the GST family proteins that we found to be upregulated in acentrosomal cells have also previously been found to be upregulated when KEAP1-Nrf2 signaling is experimentally activated (LOBODA *et al.* 2016). Indeed, the Drosophila

Nrf2 homolog, Cap-n-collar (Cnc), was recently proposed to help limit ROS levels in the wing disc following tissue damage induced by Rpr misexpression (BROCK *et al.* 2017). In their model, increased ROS levels activate Cnc, which negatively regulates ROS levels via increased transcription of ROS suppressors. They also suggest that this Cnc-mediated mechanism to restrict ROS levels helps maintain an optimal level of JNK signaling needed for tissue repair and development. Our attempts to disrupt KEAP1-Nrf2 signaling in our RNAi-based genetic interaction screen did not reveal any significant genetic interactions with *sas-4* knockdown (Table 5). However, whether that is due to true lack of functional interaction or a simple lack of effective knockdown remains unclear. Nevertheless, our data suggest that, G6PD upregulation serves as an important buffer against excessive ROS levels—reducing G6PD levels in acentrosomal cells significantly increases ROS levels above that induced by centrosome loss alone. Furthermore, apoptosis is elevated after loss of G6PD in acentrosomal cells, perhaps due to the increased levels of ROS. Induction of antioxidant-promoting proteins like G6PD and the GST proteins may be a part of a response by which lower levels of JNK induced in not yet apoptotic cells may allow them to survive and correct minor mitotic errors—similar to the response in neighboring cells induced by extracellular ROS (SANTABARBARA-RUIZ *et al.* 2015; FOGARTY *et al.* 2016). In contrast, the higher levels of ROS associated with loss of G6PD in acentrosomal cells may lead to higher, intolerable levels of JNK activity that pushes them down the apoptotic pathway.

Centrosome loss, immunity, and xenobiotic detoxification

There are some remaining mysteries in the sets of genes upregulated after centrosome loss. We expected to see JNK pathway target genes, based on our earlier work, and the genes involved in the oxidative stress response and in apoptosis also seem reasonable based on the literature. However, two of the other most prominent gene sets were more puzzling: the upregulated list included many genes involved innate immunity and in in the xenobiotic response to toxic compounds (Table 3 and 6). As we considered this, we were made aware of previous work by the Ruvkun lab in C. elegans that suggests intriguing interpretations of our data. The Ruvkun group, in the course of an unrelated RNAi screen, noted a common response to knockdown of genes involved in certain core biological processes, including

protein translation, proteasome function, mitochondrial function and mRNA processing (MELO AND RUVKUN 2012). Knockdown of critical components of any of these led to activation of both the innate immune and the xenobiotic detoxification responses. They and others found that similar effects were induced by pathogens or by pathogen derived or natural toxins (DUNBAR *et al.* 2012; MCEWAN *et al.* 2012; GOVINDAN *et al.* 2015). Based on these data, Melo and Ruvkun developed the intriguing hypothesis that animals evolved a conserved mechanism to detect and respond to pathogen attack on key cellular machines. Many pathogens encode small molecule or protein effectors that inhibit the function of these machines. In their hypothesis, cells thus evolved to respond to defects in the function of a key cellular machines by upregulating genes involved in the innate immune and the xenobiotic detoxification responses.

Our data fit well with this hypothesis. We saw upregulation of components of all three phases of the xenobiotic detoxification response, as well as many factors involved in or activated by the innate immune response (Table 3 and 6). Others have seen similar changes in response to other stresses, including the response to xenobiotic drugs like phenobarbital (MISRA *et al.* 2011) and the response to pathogenic protein aggregation (DIALYNAS *et al.* 2015; ZHAN *et al.* 2015). The genes upregulated after inactivation of the SAC also include a number encoding proteins involved in the xenobiotic response (CLEMENTE-RUIZ *et al.* 2016). Intriguing, oxidative stress also induces many of these genes (MISRA *et al.* 2011; KUCINSKI *et al.* 2017), including both ones with known antioxidant roles and those, like cytochrome p450s, without known roles in this process. Another striking parallel with the data from the Ruvkun lab is the role of the JNK pathway. They found that the responses to knockdown of genes involved in core biological processes was mediated the JNK pathway (MELO AND RUVKUN 2012), as is the case for the response to centrosome loss.

Our upregulated gene list also showed strong overlap with genes upregulated after wounding and during imaginal disc regeneration. Classic developmental biology experiments revealed that imaginal discs have a remarkable ability to regenerate after surgical or radiation damage (HAYNIE AND BRYANT 1977), by a process now known as compensatory proliferation (FAN AND BERGMANN 2008). This response also requires the JNK pathway. Strikingly, when examining the list of genes upregulated during early stages

regeneration (KATSUYAMA *et al.* 2015), nine of the top twenty are also significantly upregulated after knockdown of both *sas-4* or *asl*. Thus, the genes upregulated after surgical injury and those induced by programmed cell death after centrosome loss are strikingly similar. Many of these upregulated genes are part of the generalized wound response, such as MMP1 and PGRP-SA (PATTERSON *et al.* 2013), suggesting that at least part of these transcriptional responses are parallel ones. The genes upregulated after disc regeneration also included genes involved in the xenobiotic response (e.g. three Cytochrome p450 genes and seven GST family members), suggesting the possibility that animals are genetically programmed to interpret tissue injury as a pathogen attack.

Together, our previous and current data demonstrate the robust and multi-layered mechanisms that help cells and tissues compensate for the absence of centrosomes. In proliferating epithelia, such as the wing imaginal disc, alternative microtubule nucleation pathways help build mitotic spindles, and the Spindle Assembly Checkpoint slows mitotic progression to facilitate these less-efficient pathways (POULTON *et al.* 2014). Although many cells appear to divide without obvious mitotic error, a significant number of them suffer defects related to chromosome segregation errors (e.g., lagging chromosomes, aneuploidy, and DNA damage). Our data and others suggest it is these cells that activate high levels of JNK signaling, which drives those cells into the apoptotic pathway (DEKANTY *et al.* 2012; POULTON *et al.* 2014). JNK also acts as a homeostatic buffer in the tissue by promoting compensatory proliferation in the neighboring cells (IGAKI 2009). In the present study, we uncovered an additional consequence of centrosome loss, increased ROS, and another compensatory process, upregulation of oxidative stress response genes like *g6pd*. A growing body of recent work has begun to reveal a complex network of signaling pathways and cellular processes that link cellular defects, such as mitotic errors and subsequent activation of JNK signaling and apoptosis, to oxidative stress and compensatory proliferation/regeneration. The relationships among these players is not yet fully understood, in part due to the complexity that has emerged from recent studies, including bi-directionality (e.g., ROS ←→ JNK), tissue-specific mechanisms (e.g., eye disc vs wing disc), and threshold-dependent responses (e.g., JNK promoting apoptosis vs. survival/proliferation). Future studies will help further characterize the circuitry defining

these relationships and the underlying causes for the apparent specificity of some mechanisms.

Methods

Drosophila genetics

The following fly stocks were used: *y w* (Bloomington Drosophila Stock Center (BDSC) #1495) was used as the WT control; *sas-4*^{S2214} (BDSC #12119), *asl*^{mecD} (Blachon et al., 2008), *UAS-sas-4 RNAi* (BDSC #35049), *UAS-mud RNAi* (BDSC #35044), *UAS-bub3 RNAi* (BDSC #32989), *UAS-g6pd RNAi* (Vienna Drosophila Resource Center (VDRC) #101507), *ap-Gal4 UAS-GFP* (a gift from Y. Tamori, Hokkaido University), *MS1096-Gal4* (BDSC #8860), *en-Gal4 UAS-RFP* (BDSC #30557), *UAS bskDN* (Adachi-Yamada et al., 1999), *TRE-GFP* (CHATTERJEE AND BOHMANN 2012), *His2Av:eGFP* (BDSC #24163), *UAS-p35* (BDSC #5072), *UAS-g6pd[9g]* (LEGAN *et al.* 2008), *GSTD1>GFP* (SYKIOTIS AND BOHMANN 2008), *Ilp8:GFP*^{MI00727} (BDSC #33079). A list of additional RNAi stocks tested in the candidate gene screen can be found in Table 5.

Detection and quantification of ROS levels

To determine ROS levels, we stained the indicated genotypes with DHE (Millipore) using the following protocol; modified from (OWUSU-ANSAH *et al.* 2008). Wandering 3rd instar larvae were hemi-dissected in room temperature Schneider's media with Pen/Strep. The inverted carcasses were immediately transferred to 1mL of Schneider's with 30µM DHE and incubated for 10min on a nutator at room temp. The DHE solution was removed and the carcasses were washed 3x for 2min each with Schneider's media. The wing discs were then fully dissected from the carcasses, mounted in Halocarbon oil, and immediately imaged on a Zeiss LSM Pascal confocal microscope. The same protocol was used for MitoSOX staining (5µM; Thermofisher).

To quantify and statistically compare ROS levels in the different genotypes, we used maximum intensity projections of z-stack images of DHE stainings. We then isolated and extracted the GFP+ area of the wing pouch-hinge region (i.e. the dorsal region expressing ap-Gal4 driven transgenes of interest), measured the area of the selected region, and counted the number of DHE+ cells. Because of inter-experimental variability

associated with live sample preps and DHE staining, it is not possible to quantitatively compare DHE levels among different genotypes. To circumvent this issue, we used the ventral region of the wing disc as a control by which to standardize the DHE signal—the ventral compartment is homozygous *sas-4* mutant but does not express any of the indicated transgenes , and thus is GFP-negative. As with the dorsal region, we measured the area of the ventral wing pouch-hinge region and counted the number of DHE+ cells. We then calculated the number of DHE+ cells/area for both the dorsal (GFP+) and ventral (GFP-) regions and divided the dorsal by the ventral. Increased or decreased ROS levels induced by transgenes expression in the dorsal region will therefore alter the ratio of dorsal:ventral DHE+ cells, with each compartment separately standardized by its area. We then used Student's t-test (Excel; two-sided, unequal variance) to determine any significant differences in means, comparing transgenic backgrounds to the *ap>GFP/+;sas-4* background.

RNA-Seq experiment and analysis

Total RNA was isolated from wing imaginal discs from wandering larvae as described previously (McKay and Lieb 2013). RNA from 20 larval wing discs of a given genotype was isolated. This process was repeated 3 times per genotype to yield 3 biological replicates. RNA-Sequencing was performed by the UNC High-Throughput Sequencing Facility. Libraries were created using the TruSeq Stranded mRNA kit from Illumina. Reads were aligned to the annotated dm3 *Drosophila* genome using TopHat (v2.0.14)(Trapnell *et al.* 2012). Read depth for each gene was generated using the Bedtools 'coverageBed' and 'groupBy' tools. Differential gene expression analysis was performed with edgeR (version 3.14.0). Differentially-expressed genes were defined as having an FDR less than or equal to 0.001, and having an average FPKM value greater than or equal to 10 in at least one sample. Gene ontology analysis was performed using DAVID (version 6.8). Motif enrichment analysis was performed using AME (McLeay and Bailey 2010), in combination with transcription factor motifs from the Fly Factor Survey database. *De novo* motif discovery was performed using DREME (Bailey 2011). Additional details are available upon request. Graphical displays of RNA-Seq data used in figures were generated from the UCSC Genome Browser, or using edgeR's estimates of RNA abundance.

Immunocytochemistry and Imaging

Wing disc fixation and antibody staining were performed as previously described (ROBERTS *et al.* 2012); briefly 3rd instar larvae were fixed for 20min in 4%PFA, washed 3x with 0.1%PBT, blocked with PBT plus goat serum, incubated overnight in primary antibodies, washed 3x with PBT, incubated with secondary antibodies, washed 3x with PBT, then mounted in Aquapolymount. Antibodies used: cleaved Caspase3 (1:200, Cell Signaling), MMP1 (1:50, DSHB), Jra (1:500, Santa Cruz). Alexa secondary antibodies were used at 1:500. Phalloidin was spiked into secondary antibodies at 1:500. Confocal images were acquired on a Zeiss Pascal microscope. PhotoshopCS4 (Adobe) was used to adjust levels so the range of signals spanned the entire output grayscale and to adjust brightness and contrast. Adult wing images were acquired on a Samsung Galaxy S8 attached to a Unitron FS30 microscope.

Acknowledgements

We thank D. Bohmann, W. Orr, Y. Tamori, L. Wallrath, Bloomington Drosophila Stock Center, Vienna Drosophila Resource Center, and Developmental Studies Hybridoma Bank for reagents, J. Cuningham for technical assistance, S. Nystrom for assistance with motif analysis, T. Perdue for assistance in microscopy, the UNC High-Throughput Sequencing Facility, and our UNC colleagues for excellent suggestions. The authors declare no competing financial interests. The work was supported by NIH R35 GM118096 to MP, Research Scholar Grant 17-164-01-DDC from the American Cancer Society to DJM, and startup funds from UNC's Department of Medicine to JSP.

References

Bachhawat, A. K., and S. Yadav, 2018 The glutathione cycle: Glutathione metabolism beyond the gamma-glutamyl cycle. IUBMB Life 70**:** 585-592.

Bailey, T. L., 2011 DREME: motif discovery in transcription factor ChIP-seq data. Bioinformatics 27**:** 1653-1659.

Basto, R., J. Lau, T. Vinogradova, A. Gardiol, C. G. Woods *et al.*, 2006 Flies without centrioles. Cell 125**:** 1375-1386.

Baumbach, J., M. P. Levesque and J. W. Raff, 2012 Centrosome loss or amplification does not dramatically perturb global gene expression in Drosophila. Biol Open 1**:** 983-993.

Bazzi, H., and K. V. Anderson, 2014 Acentriolar mitosis activates a p53-dependent apoptosis pathway in the mouse embryo. Proc Natl Acad Sci U S A 111**:** E1491-1500.

Beira, J. V., and R. Paro, 2016 The legacy of Drosophila imaginal discs. Chromosoma 125**:** 573-592.

Bindokas, V. P., J. Jordan, C. C. Lee and R. J. Miller, 1996 Superoxide production in rat hippocampal neurons: selective imaging with hydroethidine. J Neurosci 16**:** 1324-1336.

Blachon, S., J. Gopalakrishnan, Y. Omori, A. Polyanovsky, A. Church *et al.*, 2008 Drosophila asterless and vertebrate Cep152 Are orthologs essential for centriole duplication. Genetics 180**:** 2081-2094.

Board, P. G., and D. Menon, 2013 Glutathione transferases, regulators of cellular metabolism and physiology. Biochim Biophys Acta 1830**:** 3267-3288.

Bond, D., and E. Foley, 2009 A quantitative RNAi screen for JNK modifiers identifies Pvr as a novel regulator of Drosophila immune signaling. PLoS Pathog 5**:** e1000655.

Borges, H. L., R. Linden and J. Y. Wang, 2008 DNA damage-induced cell death: lessons from the central nervous system. Cell Res 18**:** 17-26.

Boutros, M., H. Agaisse and N. Perrimon, 2002 Sequential activation of signaling pathways during innate immune responses in Drosophila. Dev Cell 3**:** 711-722.

Brock, A. R., M. Seto and R. K. Smith-Bolton, 2017 Cap-n-Collar Promotes Tissue Regeneration by Regulating ROS and JNK Signaling in the Drosophila melanogaster Wing Imaginal Disc. Genetics 206**:** 1505-1520.

Buchon, N., N. A. Broderick, M. Poidevin, S. Pradervand and B. Lemaitre, 2009 Drosophila intestinal response to bacterial infection: activation of host defense and stem cell proliferation. Cell Host Microbe 5**:** 200-211.

Buchon, N., N. Silverman and S. Cherry, 2014 Immunity in Drosophila melanogaster--from microbial recognition to whole-organism physiology. Nat Rev Immunol 14**:** 796-810.

Bunker, B. D., T. T. Nellimoottil, R. M. Boileau, A. K. Classen and D. Bilder, 2015 The transcriptional response to tumorigenic polarity loss in Drosophila. Elife 4.

Camhi, S. L., P. Lee and A. M. Choi, 1995 The oxidative stress response. New Horiz 3**:** 170-182.

Campos, I., J. A. Geiger, A. C. Santos, V. Carlos and A. Jacinto, 2010 Genetic screen in Drosophila melanogaster uncovers a novel set of genes required for embryonic epithelial repair. Genetics 184**:** 129-140.

Chatterjee, A., and S. Gupta, 2018 The multifaceted role of glutathione S-transferases in cancer. Cancer Lett 433**:** 33-42.

Chatterjee, N., and D. Bohmann, 2012 A versatile PhiC31 based reporter system for measuring AP-1 and Nrf2 signaling in Drosophila and in tissue culture. PLoS One 7**:** e34063.

Chen, R., M. Xu, J. Nagati and J. A. Garcia, 2017 Coordinate regulation of stress signaling and epigenetic events by Acss2 and HIF-2 in cancer cells. PLoS One 12**:** e0190241.

Christmann, M., and B. Kaina, 2013 Transcriptional regulation of human DNA repair genes following genotoxic stress: trigger mechanisms, inducible responses and genotoxic adaptation. Nucleic Acids Res 41**:** 8403-8420.

Clarke, P. R., and C. Zhang, 2008 Spatial and temporal coordination of mitosis by Ran GTPase. Nat Rev Mol Cell Biol 9**:** 464-477.

Clemente-Ruiz, M., J. M. Murillo-Maldonado, N. Benhra, L. Barrio, L. Perez *et al.*, 2016 Gene Dosage Imbalance Contributes to Chromosomal Instability-Induced Tumorigenesis. Dev Cell 36**:** 290-302.

Colombani, J., D. S. Andersen and P. Leopold, 2012 Secreted peptide Dilp8 coordinates Drosophila tissue growth with developmental timing. Science 336**:** 582-585.

Dekanty, A., L. Barrio, M. Muzzopappa, H. Auer and M. Milan, 2012 Aneuploidy-induced delaminating cells drive tumorigenesis in Drosophila epithelia. Proc Natl Acad Sci U S A 109**:** 20549-20554.

Dhanasekaran, D. N., and E. P. Reddy, 2017 JNK-signaling: A multiplexing hub in programmed cell death. Genes Cancer 8**:** 682-694.

Dialynas, G., O. K. Shrestha, J. M. Ponce, M. Zwerger, D. A. Thiemann *et al.*, 2015 Myopathic lamin mutations cause reductive stress and activate the nrf2/keap-1 pathway. PLoS Genet 11**:** e1005231.

Dobbelaere, J., F. Josue, S. Suijkerbuijk, B. Baum, N. Tapon *et al.*, 2008 A genome-wide RNAi screen to dissect centriole duplication and centrosome maturation in Drosophila. PLoS Biol 6**:** e224.

Dostert, C., E. Jouanguy, P. Irving, L. Troxler, D. Galiana-Arnoux *et al.*, 2005 The Jak-STAT signaling pathway is required but not sufficient for the antiviral response of drosophila. Nat Immunol 6**:** 946-953.

Dunbar, T. L., Z. Yan, K. M. Balla, M. G. Smelkinson and E. R. Troemel, 2012 C. elegans detects pathogen-induced translational inhibition to activate immune signaling. Cell Host Microbe 11**:** 375-386.

Fan, Y., and A. Bergmann, 2008 Apoptosis-induced compensatory proliferation. The Cell is dead. Long live the Cell! Trends Cell Biol 18**:** 467-473.

Ferguson, L. C., J. Green, A. Surridge and C. D. Jiggins, 2011 Evolution of the insect yellow gene family. Mol Biol Evol 28**:** 257-272.

Fogarty, C. E., N. Diwanji, J. L. Lindblad, M. Tare, A. Amcheslavsky *et al.*, 2016 Extracellular Reactive Oxygen Species Drive Apoptosis-Induced Proliferation via Drosophila Macrophages. Curr Biol 26**:** 575-584.

Gao, H., X. Wu, L. Simon and N. Fossett, 2014 Antioxidants maintain E-cadherin levels to limit Drosophila prohemocyte differentiation. PLoS One 9**:** e107768.

Garelli, A., A. M. Gontijo, V. Miguela, E. Caparros and M. Dominguez, 2012 Imaginal discs secrete insulin-like peptide 8 to mediate plasticity of growth and maturation. Science 336**:** 579-582.

Gauron, C., C. Rampon, M. Bouzaffour, E. Ipendey, J. Teillon *et al.*, 2013 Sustained production of ROS triggers compensatory proliferation and is required for regeneration to proceed. Sci Rep 3**:** 2084.

Govindan, J. A., E. Jayamani, X. Zhang, P. Breen, J. Larkins-Ford *et al.*, 2015 Lipid signalling couples translational surveillance to systemic detoxification in Caenorhabditis elegans. Nat Cell Biol 17**:** 1294-1303.

Griffis, E. R., N. Stuurman and R. D. Vale, 2007 Spindly, a novel protein essential for silencing the spindle assembly checkpoint, recruits dynein to the kinetochore. J Cell Biol 177**:** 1005-1015.

Gruenewald, C., J. A. Botella, F. Bayersdorfer, J. A. Navarro and S. Schneuwly, 2009 Hyperoxia-induced neurodegeneration as a tool to identify neuroprotective genes in Drosophila melanogaster. Free Radic Biol Med 46**:** 1668-1676.

Hanahan, D., and R. A. Weinberg, 2011 Hallmarks of cancer: the next generation. Cell 144**:** 646-674.

Hara, N., K. Yamada, T. Shibata, H. Osago, T. Hashimoto *et al.*, 2007 Elevation of cellular NAD levels by nicotinic acid and involvement of nicotinic acid phosphoribosyltransferase in human cells. J Biol Chem 282**:** 24574-24582.

Hausheer, F. H., A. R. Parker, P. N. Petluru, K. W. Jair, S. Chen *et al.*, 2011 Mechanistic study of BNP7787-mediated cisplatin nephroprotection: modulation of human aminopeptidase N. Cancer Chemother Pharmacol 67**:** 381-391.

Hayakawa, J., S. Mittal, Y. Wang, K. S. Korkmaz, E. Adamson *et al.*, 2004 Identification of promoters bound by c-Jun/ATF2 during rapid large-scale gene activation following genotoxic stress. Mol Cell 16**:** 521-535.

Haynie, J. L., and P. J. Bryant, 1977 The effects of X-rays on the proliferation dynamics of cells in the imaginal wing disc ofDrosophila melanogaster. Wilehm Roux Arch Dev Biol 183**:** 85-100.

Hayward, D., J. Metz, C. Pellacani and J. G. Wakefield, 2014 Synergy between multiple microtubule-generating pathways confers robustness to centrosome-driven mitotic spindle formation. Dev Cell 28**:** 81-93.

Hegan, P. S., V. Mermall, L. G. Tilney and M. S. Mooseker, 2007 Roles for Drosophila melanogaster myosin IB in maintenance of enterocyte brush-border structure and resistance to the bacterial pathogen Pseudomonas entomophila. Mol Biol Cell 18**:** 4625-4636.

Hoffmann, U., and H. K. Kroemer, 2004 The ABC transporters MDR1 and MRP2: multiple functions in disposition of xenobiotics and drug resistance. Drug Metab Rev 36**:** 669-701.

Homsy, J. G., H. Jasper, X. G. Peralta, H. Wu, D. P. Kiehart *et al.*, 2006 JNK signaling coordinates integrin and actin functions during Drosophila embryogenesis. Dev Dyn 235**:** 427-434.

Huang da, W., B. T. Sherman and R. A. Lempicki, 2009 Systematic and integrative analysis of large gene lists using DAVID bioinformatics resources. Nat Protoc 4**:** 44-57.

Hull-Thompson, J., J. Muffat, D. Sanchez, D. W. Walker, S. Benzer *et al.*, 2009 Control of metabolic homeostasis by stress signaling is mediated by the lipocalin NLaz. PLoS Genet 5**:** e1000460.

Huu, N. T., H. Yoshida and M. Yamaguchi, 2015 Tumor suppressor gene OSCP1/NOR1 regulates apoptosis, proliferation, differentiation, and ROS generation during eye development of Drosophila melanogaster. FEBS J 282**:** 4727-4746.

Igaki, T., 2009 Correcting developmental errors by apoptosis: lessons from Drosophila JNK signaling. Apoptosis 14**:** 1021-1028.

Indo, H. P., C. L. Hawkins, I. Nakanishi, K. I. Matsumoto, H. Matsui *et al.*, 2017 Role of Mitochondrial Reactive Oxygen Species in the Activation of Cellular Signals, Molecules, and Function. Handb Exp Pharmacol 240**:** 439-456.

Ishimaru, S., R. Ueda, Y. Hinohara, M. Ohtani and H. Hanafusa, 2004 PVR plays a critical role via JNK activation in thorax closure during Drosophila metamorphosis. EMBO J 23**:** 3984-3994.

James, M. O., and S. Ambadapadi, 2013 Interactions of cytosolic sulfotransferases with xenobiotics. Drug Metab Rev 45**:** 401-414.

Jasper, H., V. Benes, C. Schwager, S. Sauer, S. Clauder-Munster *et al.*, 2001 The genomic response of the Drosophila embryo to JNK signaling. Dev Cell 1**:** 579-586.

Kanda, H., T. Igaki, H. Okano and M. Miura, 2011 Conserved metabolic energy production pathways govern Eiger/TNF-induced nonapoptotic cell death. Proc Natl Acad Sci U S A 108**:** 18977-18982.

Katsuyama, T., F. Comoglio, M. Seimiya, E. Cabuy and R. Paro, 2015 During Drosophila disc regeneration, JAK/STAT coordinates cell proliferation with Dilp8-mediated developmental delay. Proc Natl Acad Sci U S A 112**:** E2327-2336.

Khan, S. J., S. N. F. Abidi, A. Skinner, Y. Tian and R. K. Smith-Bolton, 2017 The Drosophila Duox maturation factor is a key component of a positive feedback loop that sustains regeneration signaling. PLoS Genet 13**:** e1006937.

Kohlmaier, G., J. Loncarek, X. Meng, B. F. McEwen, M. M. Mogensen *et al.*, 2009 Overly long centrioles and defective cell division upon excess of the SAS-4-related protein CPAP. Curr Biol 19**:** 1012-1018.

Kondo, S., N. Senoo-Matsuda, Y. Hiromi and M. Miura, 2006 DRONC coordinates cell death and compensatory proliferation. Mol Cell Biol 26**:** 7258-7268.

Kucerova, L., O. I. Kubrak, J. M. Bengtsson, H. Strnad, S. Nylin *et al.*, 2016 Slowed aging during reproductive dormancy is reflected in genome-wide transcriptome changes in Drosophila melanogaster. BMC Genomics 17**:** 50.

Kucinski, I., M. Dinan, G. Kolahgar and E. Piddini, 2017 Chronic activation of JNK JAK/STAT and oxidative stress signalling causes the loser cell status. Nat Commun 8**:** 136.

Kundu, T. K., M. Velayutham and J. L. Zweier, 2012 Aldehyde oxidase functions as a superoxide generating NADH oxidase: an important redox regulated pathway of cellular oxygen radical formation. Biochemistry 51**:** 2930-2939.

La Fortezza, M., M. Schenk, A. Cosolo, A. Kolybaba, I. Grass *et al.*, 2016 JAK/STAT signalling mediates cell survival in response to tissue stress. Development 143**:** 2907-2919.

Lee, W. J., and M. Miura, 2014 Mechanisms of systemic wound response in Drosophila. Curr Top Dev Biol 108**:** 153-183.

Legan, S. K., I. Rebrin, R. J. Mockett, S. N. Radyuk, V. I. Klichko *et al.*, 2008 Overexpression of glucose-6-phosphate dehydrogenase extends the life span of Drosophila melanogaster. J Biol Chem 283**:** 32492-32499.

Lerit, D. A., H. A. Jordan, J. S. Poulton, C. J. Fagerstrom, B. J. Galletta *et al.*, 2015 Interphase centrosome organization by the PLP-Cnn scaffold is required for centrosome function. J Cell Biol 210**:** 79-97.

Lerit, D. A., and J. S. Poulton, 2016 Centrosomes are multifunctional regulators of genome stability. Chromosome Res 24**:** 5-17.

Lian, J., R. Nelson and R. Lehner, 2018 Carboxylesterases in lipid metabolism: from mouse to human. Protein Cell 9**:** 178-195.

Loboda, A., M. Damulewicz, E. Pyza, A. Jozkowicz and J. Dulak, 2016 Role of Nrf2/HO-1 system in development, oxidative stress response and diseases: an evolutionarily conserved mechanism. Cell Mol Life Sci 73**:** 3221-3247.

Logarinho, E., T. Resende, C. Torres and H. Bousbaa, 2008 The human spindle assembly checkpoint protein Bub3 is required for the establishment of efficient kinetochore-microtubule attachments. Mol Biol Cell 19**:** 1798-1813.

Lu, S. C., 2013 Glutathione synthesis. Biochim Biophys Acta 1830**:** 3143-3153.

Martin, F. A., A. Perez-Garijo and G. Morata, 2009 Apoptosis in Drosophila: compensatory proliferation and undead cells. Int J Dev Biol 53**:** 1341-1347.

Martindale, J. L., and N. J. Holbrook, 2002 Cellular response to oxidative stress: signaling for suicide and survival. J Cell Physiol 192**:** 1-15.

Massudi, H., R. Grant, N. Braidy, J. Guest, B. Farnsworth *et al.*, 2012 Age-associated changes in oxidative stress and NAD+ metabolism in human tissue. PLoS One 7**:** e42357.

McEwan, D. L., N. V. Kirienko and F. M. Ausubel, 2012 Host translational inhibition by Pseudomonas aeruginosa Exotoxin A Triggers an immune response in Caenorhabditis elegans. Cell Host Microbe 11**:** 364-374.

McKay, D. J., and J. D. Lieb, 2013 A common set of DNA regulatory elements shapes Drosophila appendages. Dev Cell 27**:** 306-318.

McLeay, R. C., and T. L. Bailey, 2010 Motif Enrichment Analysis: a unified framework and an evaluation on ChIP data. BMC Bioinformatics 11**:** 165.

Meekins, D. A., M. R. Kanost and K. Michel, 2017 Serpins in arthropod biology. Semin Cell Dev Biol 62**:** 105-119.

Melo, J. A., and G. Ruvkun, 2012 Inactivation of conserved C. elegans genes engages pathogen- and xenobiotic-associated defenses. Cell 149**:** 452-466.

Mennella, V., B. Keszthelyi, K. L. McDonald, B. Chhun, F. Kan *et al.*, 2012 Subdiffraction-resolution fluorescence microscopy reveals a domain of the centrosome critical for pericentriolar material organization. Nat Cell Biol 14**:** 1159-1168.

Misra, J. R., M. A. Horner, G. Lam and C. S. Thummel, 2011 Transcriptional regulation of xenobiotic detoxification in Drosophila. Genes Dev 25**:** 1796-1806.

Montooth, K. L., K. T. Siebenthall and A. G. Clark, 2006 Membrane lipid physiology and toxin catabolism underlie ethanol and acetic acid tolerance in Drosophila melanogaster. J Exp Biol 209**:** 3837-3850.

Morais da Silva, S., T. Moutinho-Santos and C. E. Sunkel, 2013 A tumor suppressor role of the Bub3 spindle checkpoint protein after apoptosis inhibition. J Cell Biol 201**:** 385-393.

Moussian, B., 2010 Recent advances in understanding mechanisms of insect cuticle differentiation. Insect Biochem Mol Biol 40**:** 363-375.

Moutinho-Pereira, S., N. Stuurman, O. Afonso, M. Hornsveld, P. Aguiar *et al.*, 2013 Genes involved in centrosome-independent mitotic spindle assembly in Drosophila S2 cells. Proc Natl Acad Sci U S A 110**:** 19808-19813.

Musacchio, A., 2015 The Molecular Biology of Spindle Assembly Checkpoint Signaling Dynamics. Curr Biol 25**:** R1002-1018.

Nakajima, Y., E. J. Meyer, A. Kroesen, S. A. McKinney and M. C. Gibson, 2013 Epithelial junctions maintain tissue architecture by directing planar spindle orientation. Nature 500**:** 359-362.

Nicholson, J. M., and D. Cimini, 2011 How mitotic errors contribute to karyotypic diversity in cancer. Adv Cancer Res 112**:** 43-75.

Novak, Z. A., P. T. Conduit, A. Wainman and J. W. Raff, 2014 Asterless licenses daughter centrioles to duplicate for the first time in Drosophila embryos. Curr Biol 24**:** 1276-1282.

O'Keefe, L. V., C. S. Lee, A. Choo and R. I. Richards, 2015 Tumor Suppressor WWOX Contributes to the Elimination of Tumorigenic Cells in Drosophila melanogaster. PLoS One 10**:** e0136356.

O'Rourke, D., D. Baban, M. Demidova, R. Mott and J. Hodgkin, 2006 Genomic clusters, putative pathogen recognition molecules, and antimicrobial genes are induced by infection of C. elegans with M. nematophilum. Genome Res 16**:** 1005-1016.

Oda, H., Y. Suzuki, T. Shibata and A. Yoshida, 1999 Glucocorticoid-dependent induction of HMG-CoA reductase and malic enzyme gene expression by polychlorinated biphenyls in rat hepatocytes. J Nutr Biochem 10**:** 644-653.

Ohsawa, S., Y. Sato, M. Enomoto, M. Nakamura, A. Betsumiya *et al.*, 2012 Mitochondrial defect drives non-autonomous tumour progression through Hippo signalling in Drosophila. Nature 490**:** 547-551.

Owusu-Ansah, E., A. Yavari, S. Mandal and U. Banerjee, 2008 Distinct mitochondrial retrograde signals control the G1-S cell cycle checkpoint. Nat Genet 40**:** 356-361.

Pandey, A. V., and C. E. Fluck, 2013 NADPH P450 oxidoreductase: structure, function, and pathology of diseases. Pharmacol Ther 138**:** 229-254.

Pastor-Pareja, J. C., M. Wu and T. Xu, 2008 An innate immune response of blood cells to tumors and tissue damage in Drosophila. Dis Model Mech 1**:** 144-154; discussion 153.

Patterson, R. A., M. T. Juarez, A. Hermann, R. Sasik, G. Hardiman *et al.*, 2013 Serine proteolytic pathway activation reveals an expanded ensemble of wound response genes in Drosophila. PLoS One 8**:** e61773.

Peretz, G., A. Bakhrat and U. Abdu, 2007 Expression of the Drosophila melanogaster GADD45 homolog (CG11086) affects egg asymmetric development that is mediated by the c-Jun N-terminal kinase pathway. Genetics 177**:** 1691-1702.

Perez-Garijo, A., E. Shlevkov and G. Morata, 2009 The role of Dpp and Wg in compensatory proliferation and in the formation of hyperplastic overgrowths caused by apoptotic cells in the Drosophila wing disc. Development 136**:** 1169-1177.

Perez, E., J. L. Lindblad and A. Bergmann, 2017 Tumor-promoting function of apoptotic caspases by an amplification loop involving ROS, macrophages and JNK in Drosophila. Elife 6.

Picco, V., and G. Pages, 2013 Linking JNK Activity to the DNA Damage Response. Genes Cancer 4**:** 360-368.

Poulton, J. S., J. C. Cuningham and M. Peifer, 2014 Acentrosomal Drosophila epithelial cells exhibit abnormal cell division, leading to cell death and compensatory proliferation. Dev Cell 30**:** 731-745.

Poulton, J. S., J. C. Cuningham and M. Peifer, 2017 Centrosome and spindle assembly checkpoint loss leads to neural apoptosis and reduced brain size. J Cell Biol 216**:** 1255-1265.

Prosser, S. L., and L. Pelletier, 2017 Mitotic spindle assembly in animal cells: a fine balancing act. Nat Rev Mol Cell Biol 18**:** 187-201.

Redza-Dutordoir, M., and D. A. Averill-Bates, 2016 Activation of apoptosis signalling pathways by reactive oxygen species. Biochim Biophys Acta 1863**:** 2977-2992.

Richens, J. H., T. P. Barros, E. P. Lucas, N. Peel, D. M. Pinto *et al.*, 2015 The Drosophila Pericentrin-like-protein (PLP) cooperates with Cnn to maintain the integrity of the outer PCM. Biol Open 4**:** 1052-1061.

Rios-Barrera, L. D., and J. R. Riesgo-Escovar, 2013 Regulating cell morphogenesis: the Drosophila Jun N-terminal kinase pathway. Genesis 51**:** 147-162.

Roberts, D. M., M. I. Pronobis, K. M. Alexandre, G. C. Rogers, J. S. Poulton *et al.*, 2012 Defining components of the ss-catenin destruction complex and exploring its regulation and mechanisms of action during development. PLoS One 7**:** e31284.

Rousset, R., S. Bono-Lauriol, M. Gettings, M. Suzanne, P. Speder *et al.*, 2010 The Drosophila serine protease homologue Scarface regulates JNK signalling in a negative-feedback loop during epithelial morphogenesis. Development 137**:** 2177-2186.

Ryoo, H. D., T. Gorenc and H. Steller, 2004 Apoptotic cells can induce compensatory cell proliferation through the JNK and the Wingless signaling pathways. Dev Cell 7**:** 491-501.

Santabarbara-Ruiz, P., M. Lopez-Santillan, I. Martinez-Rodriguez, A. Binagui-Casas, L. Perez *et al.*, 2015 ROS-Induced JNK and p38 Signaling Is Required for Unpaired Cytokine Activation during Drosophila Regeneration. PLoS Genet 11**:** e1005595.

Schmidt, T. I., J. Kleylein-Sohn, J. Westendorf, M. Le Clech, S. B. Lavoie *et al.*, 2009 Control of centriole length by CPAP and CP110. Curr Biol 19**:** 1005-1011.

Seeds, A. M., M. M. Tsui, C. Sunu, E. P. Spana and J. D. York, 2015 Inositol phosphate kinase 2 is required for imaginal disc development in Drosophila. Proc Natl Acad Sci U S A 112**:** 15660-15665.

Senger, K., K. Harris and M. Levine, 2006 GATA factors participate in tissue-specific immune responses in Drosophila larvae. Proc Natl Acad Sci U S A 103**:** 15957-15962.

Sies, H., C. Berndt and D. P. Jones, 2017 Oxidative Stress. Annu Rev Biochem 86**:** 715-748.

Silverman, N., R. Zhou, R. L. Erlich, M. Hunter, E. Bernstein *et al.*, 2003 Immune activation of NF-kappaB and JNK requires Drosophila TAK1. J Biol Chem 278**:** 48928-48934.

Stanton, R. C., 2012 Glucose-6-phosphate dehydrogenase, NADPH, and cell survival. IUBMB Life 64**:** 362-369.

Stevens, N. R., A. A. Raposo, R. Basto, D. St Johnston and J. W. Raff, 2007 From stem cell to embryo without centrioles. Curr Biol 17**:** 1498-1503.

Sykiotis, G. P., and D. Bohmann, 2008 Keap1/Nrf2 signaling regulates oxidative stress tolerance and lifespan in Drosophila. Dev Cell 14**:** 76-85.

Tang, H., 2009 Regulation and function of the melanization reaction in Drosophila. Fly (Austin) 3**:** 105-111.

Tang, H. W., H. M. Liao, W. H. Peng, H. R. Lin, C. H. Chen *et al.*, 2013 Atg9 interacts with dTRAF2/TRAF6 to regulate oxidative stress-induced JNK activation and autophagy induction. Dev Cell 27**:** 489-503.

Teesalu, M., B. M. Rovenko and V. Hietakangas, 2017 Salt-Inducible Kinase 3 Provides Sugar Tolerance by Regulating NADPH/NADP(+) Redox Balance. Curr Biol 27**:** 458-464.

Telci, D., and M. Griffin, 2006 Tissue transglutaminase (TG2)--a wound response enzyme. Front Biosci 11**:** 867-882.

Trapnell, C., A. Roberts, L. Goff, G. Pertea, D. Kim *et al.*, 2012 Differential gene and transcript expression analysis of RNA-seq experiments with TopHat and Cufflinks. Nat Protoc 7**:** 562-578.

Uhlirova, M., and D. Bohmann, 2006 JNK- and Fos-regulated Mmp1 expression cooperates with Ras to induce invasive tumors in Drosophila. EMBO J 25**:** 5294-5304.

Uyehara, C. M., S. L. Nystrom, M. J. Niederhuber, M. Leatham-Jensen, Y. Ma *et al.*, 2017 Hormone-dependent control of developmental timing through regulation of chromatin accessibility. Genes Dev 31**:** 862-875.

Voelzmann, A., I. Hahn, S. P. Pearce, N. Sanchez-Soriano and A. Prokop, 2016 A conceptual view at microtubule plus end dynamics in neuronal axons. Brain Res Bull 126**:** 226-237.

Walczak, C. E., and R. Heald, 2008 Mechanisms of mitotic spindle assembly and function. Int Rev Cytol 265**:** 111-158.

Wang, M. C., D. Bohmann and H. Jasper, 2003 JNK signaling confers tolerance to oxidative stress and extends lifespan in Drosophila. Dev Cell 5**:** 811-816.

Xie, H. B., A. Cammarato, N. S. Rajasekaran, H. Zhang, J. A. Suggs *et al.*, 2013 The NADPH metabolic network regulates human alphaB-crystallin cardiomyopathy and reductive stress in Drosophila melanogaster. PLoS Genet 9**:** e1003544.

Yang, H., and D. Hultmark, 2016 Tissue communication in a systemic immune response of Drosophila. Fly (Austin) 10**:** 115-122.

Zhan, L., Q. Xie and R. S. Tibbetts, 2015 Opposing roles of p38 and JNK in a Drosophila model of TDP-43 proteinopathy reveal oxidative stress and innate immunity as pathogenic components of neurodegeneration. Hum Mol Genet 24**:** 757-772.

Figure Legends

Figure 1. Centrosome loss dramatically increases apoptosis levels and JNK activity.
(A) Model of a dividing cell. A pair of centrosomes (yellow) nucleate microtubules (black lines), some of which attach to the chromosomes (blue), to form a bipolar spindle. (B-B") There is little to no apoptosis in wildtype (WT) 3rd larval instar wing discs, as reported by antibodies to cleaved Caspase 3. (C-C") In *sas-4* mutants, which lack centrosomes, many cells undergo apoptotic cell death. (D-D") The JNK transcriptional reporter, TRE>GFP, has no detectable expression at this stage in control discs. (E-E") Many of the acentrosomal cells in *sas-4* mutant wing discs have highly elevated JNK activity. All images are maximum intensity projections. Scale bars in all images represent 50µm. Red channel: Actin. Green channel: Cleaved Caspase 3 (Casp) in B,C; TRE>GFP in D,E. (F,G) RNA-Seq reads along the *sas-4* locus (F) and *asl* locus (G) in the *asl*, *sas-4*, or WT genotypes.

Figure 2. Analysis of RNA-Seq data reveals highly consistent gene up- and down-regulation and enrichment of genes near AP-1, GAGA, GATA, Lola, and STAT92E transcription factor binding sites.
(A) Plots comparing RNA-Seq replicates within a genotype demonstrate extremely high concordance. Pearson's R correlation values are shown. (B) MA plots reveal genes significantly up (red dots below midline) or downregulated (red dots above midline) in comparisons of *sas-4* to WT (left) or *asl* to WT (right). (C,C') Venn diagrams demonstrating the highly significant overlap of genes found to upregulated (C) or downregulated (C') in both *sas-4* and *asl*, relative to WT. (D) Transcription factor DNA-binding motifs significantly enriched in open chromatin sites near to genes upregulated in both *sas-4* and *asl*. p-values (rank sum test) and fraction of open chromatin peaks containing a designated motif are shown. (E) A *de novo* motif discovery of open chromatin peaks also uncovered enrichment of AP-1, GAGA, and GATA binding sites. (F) Directed analysis of open chromatin regions near the upregulated and downregulated genes common to *sas-4* and *asl* for enrichment of binding sites for AP-1, Nrf2, and STAT92E. Data are plotted as the enrichment over genomic background for each motif. Error bars represent 95% confidence intervals. Red dots indicate a p-value (Z-test) less

than 0.05. AP-1 was included as a control for this approach since we knew from our library-based directed search and the *de novo* search that AP-1 binding sites should be significantly enriched in our upregulated set of genes. We did not detect significant enrichment for Nrf2 sites using this approach. However, we did detect significant enrichment of the STAT92E-binding motif in our upregulated genes (this motif was not in the library for our directed search, represented in panel D).

Figure 3. Centrosome loss leads to upregulation of expression of JNK target genes. (A,E) RNA-Seq plot profiles of two known JNK target genes, *MMP1* (A) and *Jra* (E), for *asl*, *sas-4* and WT genotypes. Transcription direction indicated by arrowheads. (B,F) RNA-Seq mean signal (+/- s.d.) of the three biological replicates for *MMP1* (B) and *Jra* (F). (C) MMP1 protein, as visualized by antibody, has minimal expression in WT wing discs. (D) MMP1 protein levels are dramatically increased in acentrosomal *sas-4* wing discs. (G) Jra is weakly expressed in control discs, though there is significant expression in the peripodial cells (not shown in this single slice image). (H) Jra protein is increased in *sas-4* discs. (I-K) Representative adult wings from the indicated genotypes. Neither knockdown of *sas-4* alone (I) nor *jra* alone (J) perturbs wing development. However, knockdown of both *sas-4* and *jra* together produces necrotic spots in the adult wing. (L) RNA-Seq plot profiles of the *ilp8* locus for *asl*, *sas-4* and WT genotypes. (M) Mean RNA-Seq signal for *ilp8* in the three genotypes. (N) *ilp8* expression, as assessed using a protein trap line expressing GFP tagged Ilp8 under control of the *ilp8* promoter, is low in controls discs. (O) *ilp8* is upregulated in *sas-4* discs. (P) The upregulation of *ilp8* associated with centrosome loss is JNK-dependent because misexpression of BskDN in the posterior portion of *sas-4* homozygous mutant wing discs inhibits Ilp8:GFP upregulation. BskDN is driven by en>RFP (red in P; grayscale in P'). White dashed line marks the outer edge of the wing disc. Scale bars are 50µm. Images are max projections, except in G,H where single slices were used to limit the Jra signal from the peripodial cells.

Figure 4. Centrosome loss induces oxidative stress and upregulation of GST genes.

(A) List of *GST* genes significantly upregulated in *sas-4* and/or *asl* mutants. (B) RNA-Seq plot profiles of the *GstD1* locus in the three genotypes. Transcription direction indicated by arrowhead. (C) Mean RNA-Seq signal for *GstD1*. (D) Control WT wing discs have minimal expression of *GstD1*, as indicated by the reporter GstD1>GFP. (E) *sas-4* wing discs have elevated levels of GstD1>GFP. (F) In WT wing discs, ROS levels are essentially undetectable. His:GFP flies were used as WT in this experiment, and were mixed with *sas-4* mutant discs to provide an "in tube" control. (G) *sas-4* homozygous mutant wing discs showed strongly elevated ROS levels. (H) WT wing discs do not stain for MitoSOX, a marker of mitochondrially-derived super-oxide. (I) MitoSOX staining is elevated in *sas-4* mutant discs. Scale bars are 50μm.

Figure 5. Mitotic errors induced by other stimuli also elevate apoptosis and ROS levels, and blockade of either apoptosis or JNK reduces ROS production in acentrosomal cells.

(A,B) Knockdown of the mitotic spindle anchoring protein, Mud, leads to both increased apoptosis (A) and ROS (B). (C,D) Knockdown of the mitotic fidelity factor, Bub3, also increases both apoptosis (C) and ROS (D) levels. (E) *sas-4* homozygous mutant wing discs have elevated ROS levels, with slightly more DHE+ cells present in the dorsal compartment than the ventral (quantified in I); dorsal compartment marked by ap>GFP expression. This genotype also serves as a control for the subsequent experiments. (F) ROS production associated with centrosome loss (entire disc is *sas-4* mutant) is reduced by inhibiting apoptosis via p35 misexpression in the GFP+ dorsal area. (G) Misexpressing the JNK signaling inhibitor BskDN (a dominant negative form of JNK) prevents apoptosis caused by centrosome loss. (H) JNK blockade also reduces ROS levels in *sas-4* mutant discs. (I) Quantification of ROS levels in relevant genetic backgrounds (+/- s.d.). Blocking apoptosis through misexpression of p35 or bskDN in the dorsal region of *sas-4* mutant discs reduces ROS levels, relative to the ventral portion, which is *sas-4* mutant but does not express the indicated transgene. Scale bars are 50μm.

Figure 6. G6PD helps prevent apoptosis in acentrosomal cells.

(A-C) Representative adult wing from the indicated genotypes. (A) Knockdown of *sas-4* with MS1096-Gal4 has no observable effect on adult wing morphology. (A') *g6pd* knockdown has only minor effects on wing blade morphology, although the wings of these flies are held erect relative to the body. (A") Simultaneous knockdown of both *sas-4* and *g6pd* leads to significantly more wing blisters and furled wing phenotypes. (B) Quantification of effects on wing blade morphology. * The "Normal" wing category includes both the WT appearance seen in the *sas-4* RNAi wings, as well as the erect wings with normal wing blades observed in *g6pd* RNAi flies. "Furled" refers to wings that never expanded (unfurled) after eclosion. (C) Quantification of the effects of *sas-4* and *g6pd* manipulations on apoptosis levels. (D-I) Assessment of apoptosis levels in 3rd instar wing discs of indicated genotypes. (D) Control *ap-Gal4 UAS-GFP* (*ap>GFP*) wing discs have minimal apoptosis. (E) The elevated apoptosis throughout the wing pouch characteristic of *sas-4* homozygous mutants is not altered by expression of GFP in the dorsal region via ap>GFP. (F) Expression of *g6pd* RNAi using ap-Gal4 does not increase apoptosis in a WT background. (G) Expression of *g6pd* RNAi using ap-Gal4 in the *sas-4* mutant background significantly increases the incidence of apoptosis associated with centrosome loss, in the cells where *g6pd* is knocked down. (H) G6PD overexpression (OE) does not increase apoptosis in a WT background. (I) G6PD OE is not sufficient to reduce apoptosis caused by centrosome loss. Scale bars=50µm. All images are maximum intensity projections.

Figure 7. G6PD buffers acentrosomal cells against ROS production.

(A-F) Assessment of ROS levels in 3rd instar wing using DHE. (A) *ap>GFP* alone does not induce ROS. (B) *ap>GFP* also does not affect levels of ROS associated with centrosome loss (*sas-4* homozygous mutant disc). (C) *g6pd* knockdown in otherwise normal cells does not induce ROS production. (D) However, *g6pd* knockdown does elevate ROS in *sas-4* mutant cells above levels caused by centrosome loss alone. (E) G6PD overexpression (OE) does not affect baseline ROS production in WT. (F) G6PD OE significantly reduces levels of ROS in acentrosomal cells. Scale bars=50µm. All images are maximum intensity projections. (G) Quantification of the effects of *sas-4* and *g6pd* manipulations on ROS levels—see the Methods for a detailed description of these

calculations. (H) Model of the relationships between the relevant pathways, processes, and genes. Because G6PD buffers ROS levels in some cells, and because ROS can contribute to cell death, G6PD can indirectly inhibit cell death [this indirect relationship is indicated by the red repression symbol].

Suppl Figure 1. Blocking apoptosis after centrosome loss activates JAK-STAT signaling.

(A) In control wing discs (en>RFP only), JAK-STAT signaling appears active only in the outer, hinge region of the disc (blue arrow), based on expression of the 10xSTAT-GFP reporter. (B) Knockdown of *sas-4* (i.e., centrosome loss) in the posterior half of the wing disc (marked by en>RFP+), does not noticeably affect activity of the JAK-STAT pathway—notably, there is little activity in the wing pouch (red and green arrows). (C) However, when cell death associated with *sas-4* knockdown is inhibited by p35 misexpression, there is a significant increase in 10xSTAT-GFP expression, particularly in the wing pouch (red arrows). Interestingly, the largest increase in JAK-STAT activity is in wildtype anterior cells adjacent to the *sas-4* knockdown region (green arrows in C'). Scale bars=50μm. All images are maximum intensity projections.

Table 1. GO Terms enriched in genes higher in both *sas-4* and *asl*.

Gene Ontology (GO) Term analysis of genes with significantly increased expression in both *sas-4* and *asl* mutant wing discs, relative to WT, suggests upregulation of several biological pathways. Notable among them are indicators of oxidative stress. Unadjusted p-values are shown.

Table 2. Genes with known or putative roles in the oxidative stress response.

A list of oxidative stress response genes that were significantly upregulated in both *sas-4* and *asl* mutants relative to WT.

Table 3. Genes with known or inferred roles in innate immunity or wound healing.

Genes with reported roles in the innate immune response and/or wound healing that were significantly upregulated in both *sas-4* and *asl* mutants relative to WT.

Table 4. Genes related to JNK signaling.

List of genes that were upregulated in both *sas-4* and *asl* mutants relative to WT, and are either components or the JNK signaling cascade or transcriptional targets of JNK signaling.

Table 5. Candidate genes screened for interaction with *sas-4*.

Based on cellular function, a subset of genes was selected from the list of genes that were upregulated in both *sas-4* and *asl* mutants relative to WT. The stock identifiers for RNAi lines targeting the genes of interest are shown (BDSC=Bloomington Drosophila Stock Center; VDRC=Vienna Drosophila Resource Center). RNAi lines were crossed to the MS1096-Gal4 UAS-GFP (MS>GFP) wing disc driver alone and in combination with *sas-4* RNAi. G6PD knockdown alone had modest effects that were synergistically elevated in cells co-depleted of centrosomes by *sas-4* RNAi (see Figure 6A,B).

Table 6. Known or suspected xenobiotic response genes.

A list of genes that have increased expression in *sas-4* and *asl* mutants, relative to WT, and are also proposed to function in the response to xenobiotics.

Supplemental Table 1. Global gene expression data in *sas-4* and *asl* mutants compared to WT.

EdgeR results comparing RNA-Seq data from *sas-4* or *asl* mutants to WT control wing discs; sorted by FDR. *sas-4* and *asl* mutant data are located in separate Worksheets.

Supplemental Table 2. Genes up and downregulated in *sas-4* mutant wing discs.

List of genes and accompanying RNA-Seq data for genes significantly (FDR<0.001) up or downregulated in *sas-4* mutants, relative to WT; sorted by FDR. Upregulated and downregulated genes are on separate Worksheets.

Supplemental Table 3. Genes up and downregulated in *asl* mutant wing discs.

List of genes and accompanying RNA-Seq data for genes significantly (FDR<0.001) up or downregulated in *asl* mutants, relative to WT; sorted by FDR. Upregulated and downregulated genes are on separate Worksheets.

Supplemental Table 4. Genes significantly upregulated in both *sas-4* and *asl* mutant wing discs.

List of shared genes significantly upregulated in *sas-4* and *asl* mutants, relative to WT; sorted alphabetically.

Supplemental Table 5. Genes significantly downregulated in both *sas-4* and *asl* mutant wing discs.

List of shared genes significantly downregulated in *sas-4* and *asl* mutants, relative to WT; sorted alphabetically.

Figure1

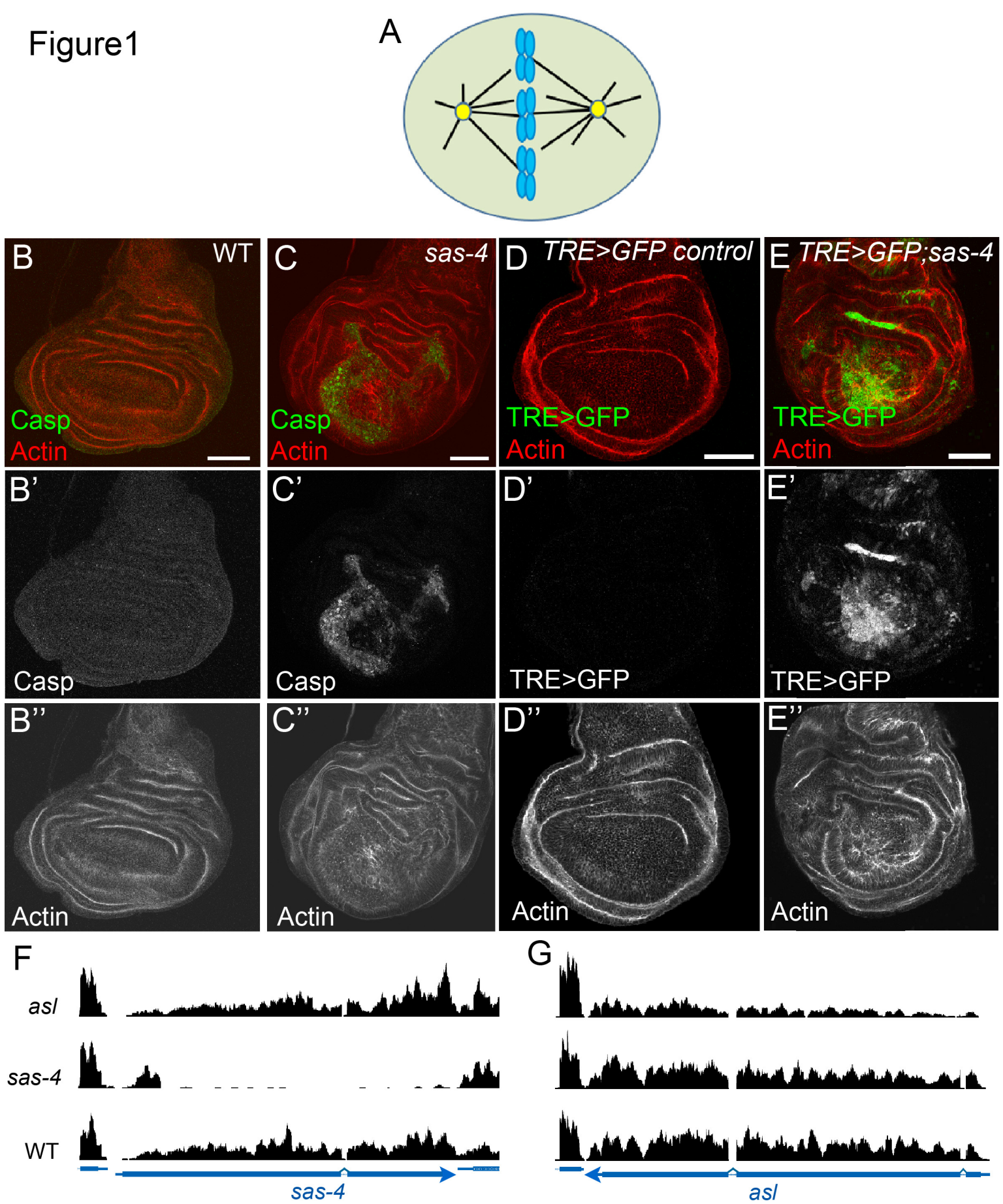
A
B
WT
Casp
Actin
C
sas-4
Casp
Actin
D
TRE>GFP control
TRE>GFP
Actin
E
TRE>GFP;sas-4
TRE>GFP
Actin
B'
Casp
C'
Casp
D'
TRE>GFP
E'
TRE>GFP
B''
Actin
C''
Actin
D''
Actin
E''
Actin
F
asl
sas-4
WT
sas-4
G
asl

Figure 2

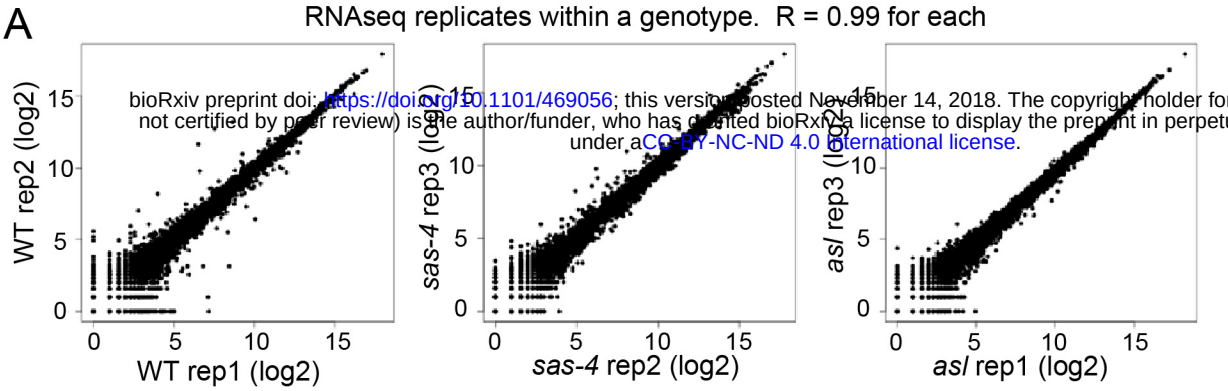

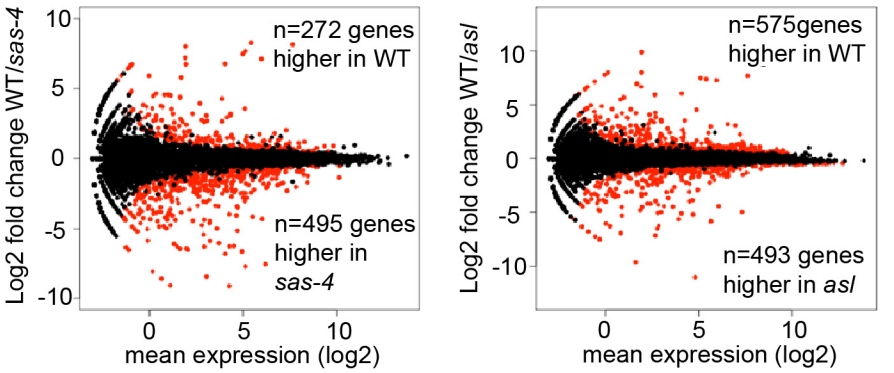

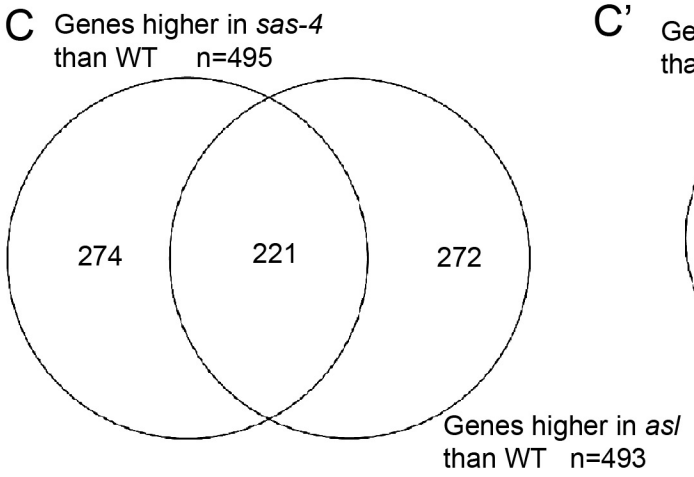

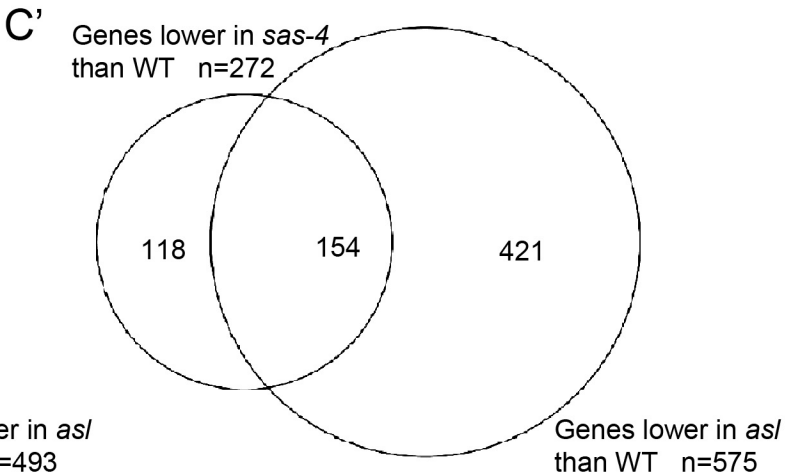

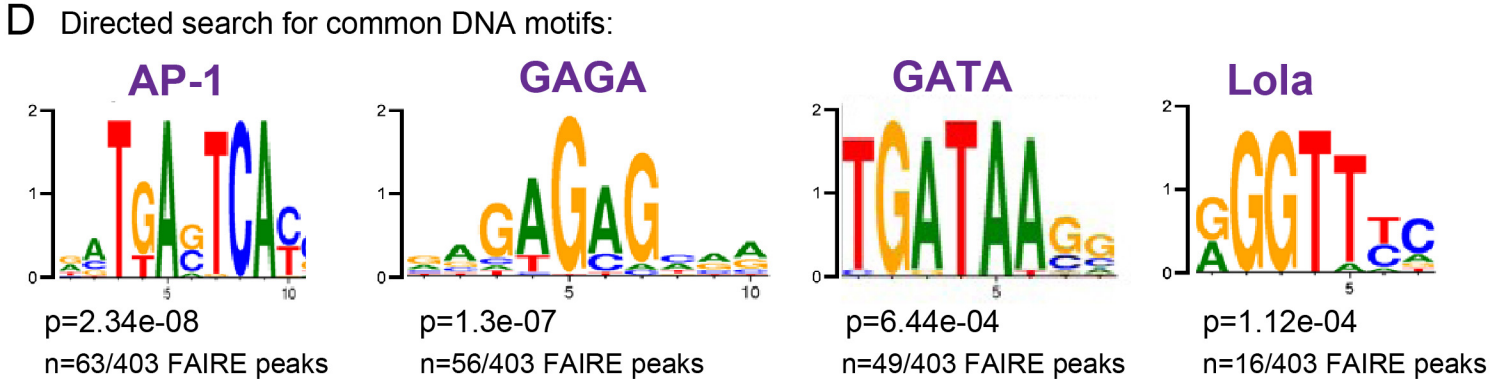

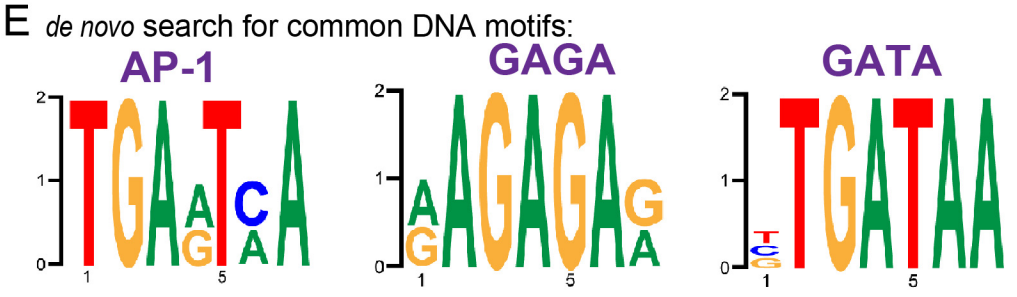

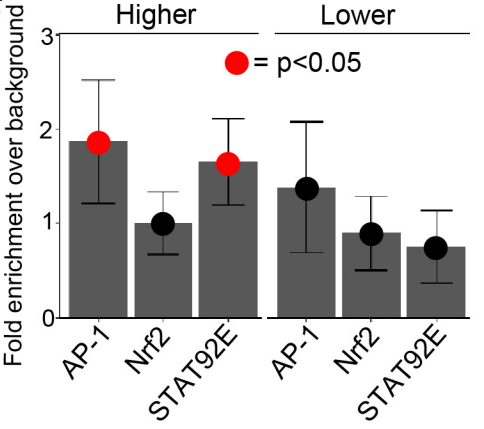

Figure3

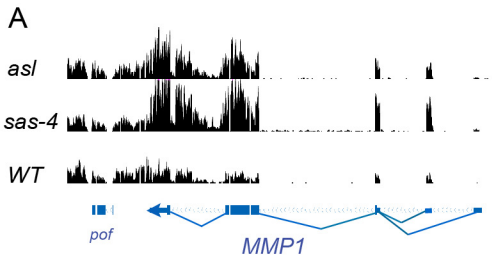

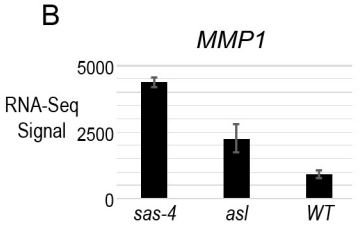

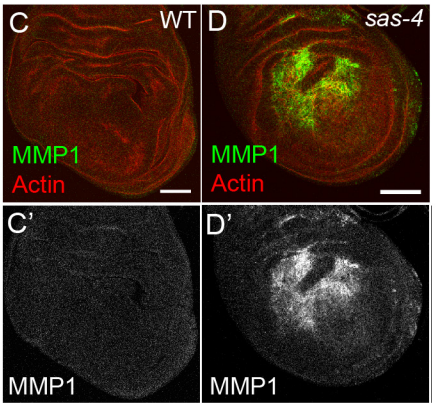

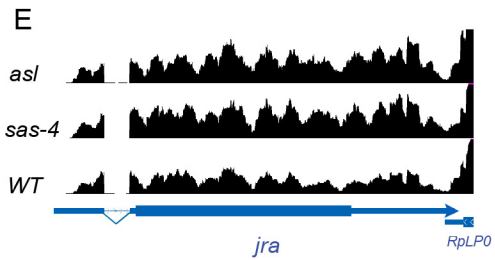

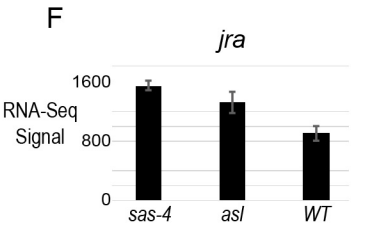

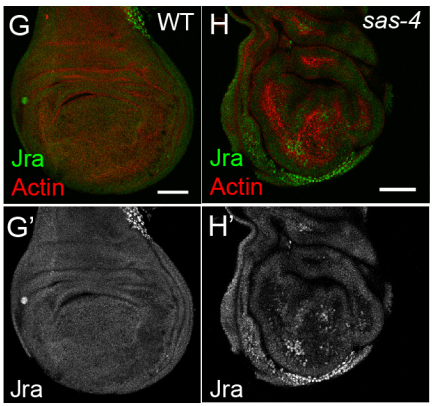

bskDN; en>RFP; Ilp8:GFP sas-4

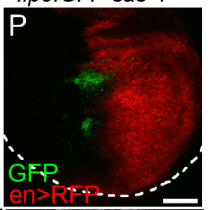

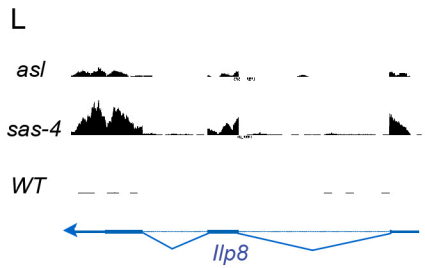

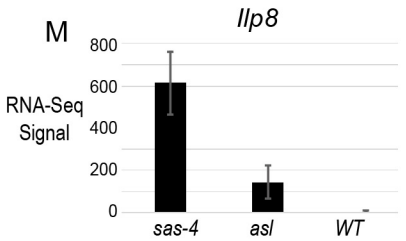

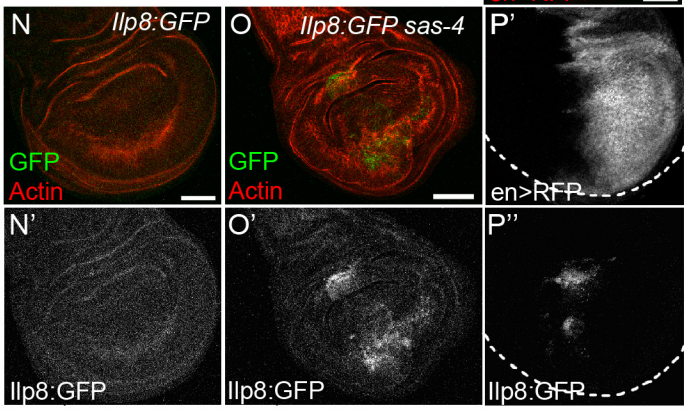

Figure 4

A

Glutathione S-transferase Genes Upregulated in *sas-4* and *asl*

Gene	Higher in *sas-4*	Higher in *asl*
GSTD1	X	X
GSTE3	X	X
GSTD3	X	X
GSTE8	X	X
GSTE6	X	X
GSTE5	X	X
GSTD2	X	
GSTD5	X	
GSTD4	X	

B

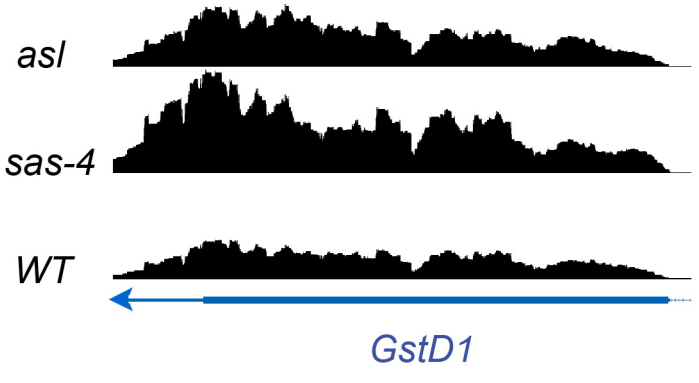

C

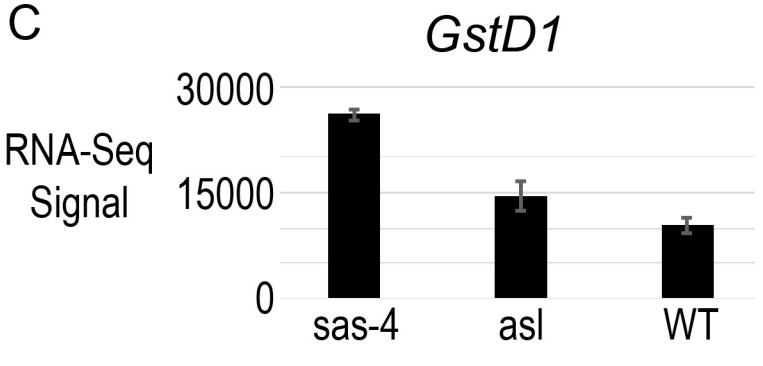

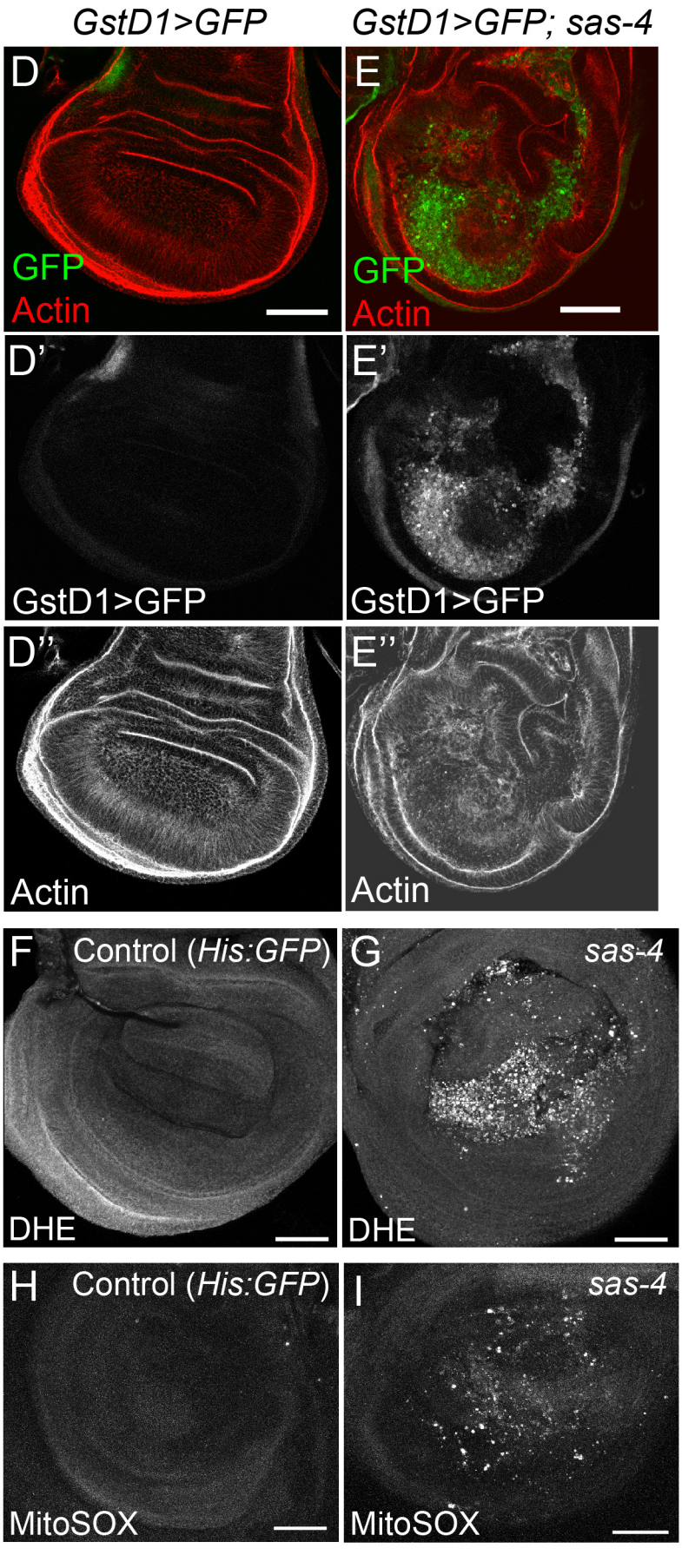

Figure 5

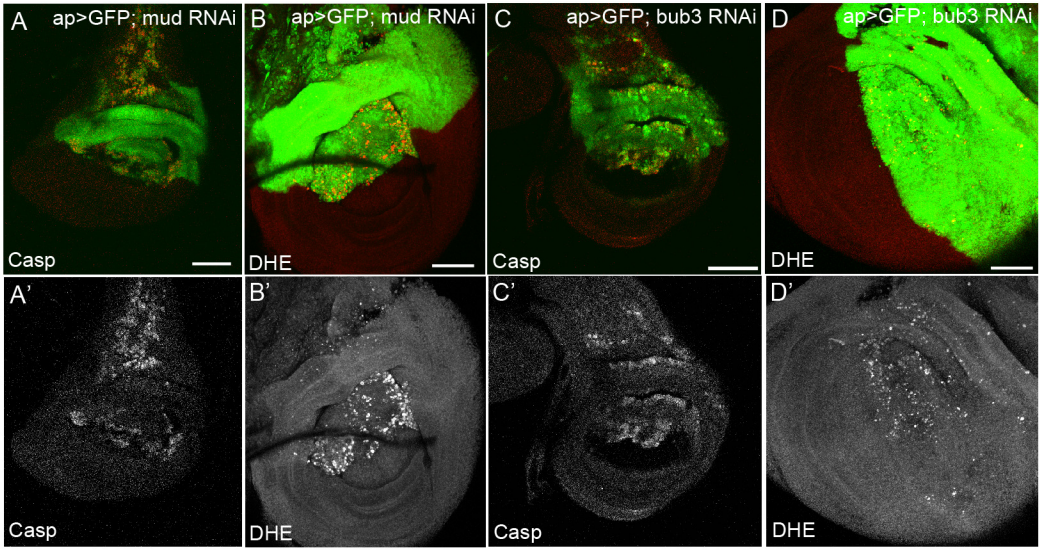
A
ap>GFP; mud RNAi
Casp
B
ap>GFP; mud RNAi
DHE
C
ap>GFP; bub3 RNAi
Casp
D
ap>GFP; bub3 RNAi
DHE
A'
Casp
B'
DHE
C'
Casp
D'
DHE

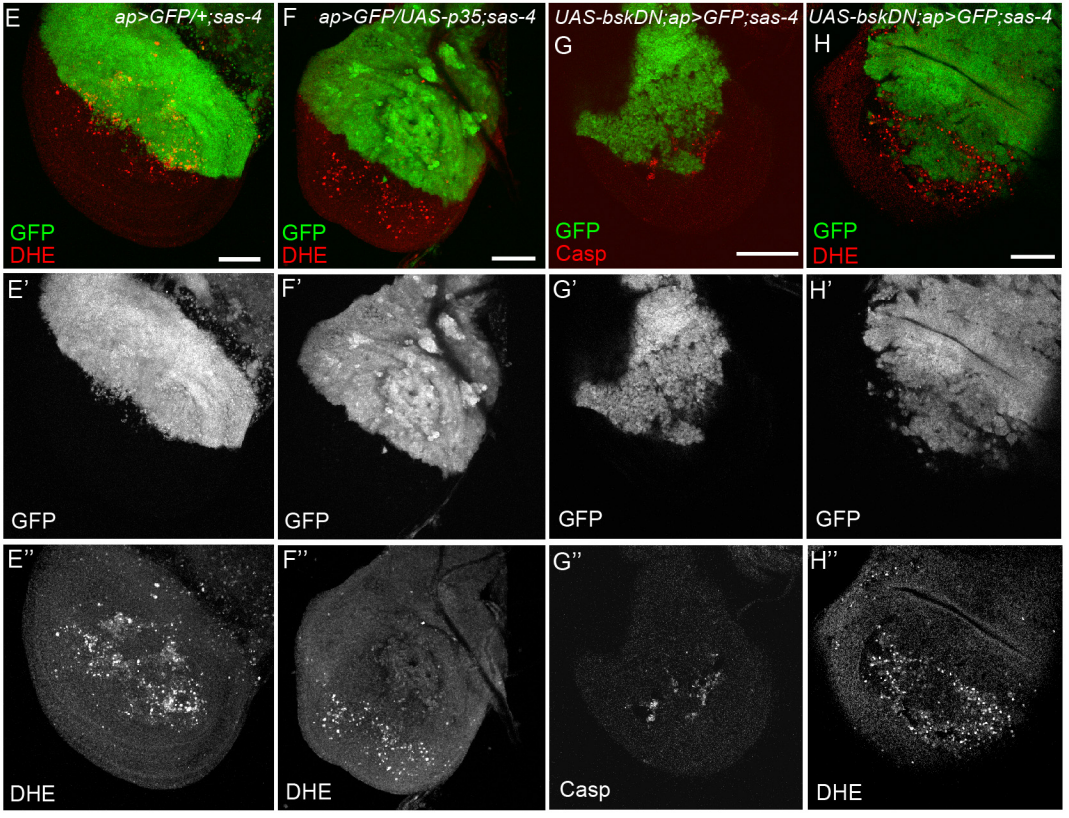
E
ap>GFP/+;sas-4
GFP
DHE
F
ap>GFP/UAS-p35;sas-4
GFP
DHE
G
UAS-bskDN;ap>GFP;sas-4
GFP
Casp
H
UAS-bskDN;ap>GFP;sas-4
GFP
DHE
E'
GFP
F'
GFP
G'
GFP
H'
GFP
E''
DHE
F''
DHE
G''
Casp
H''
DHE

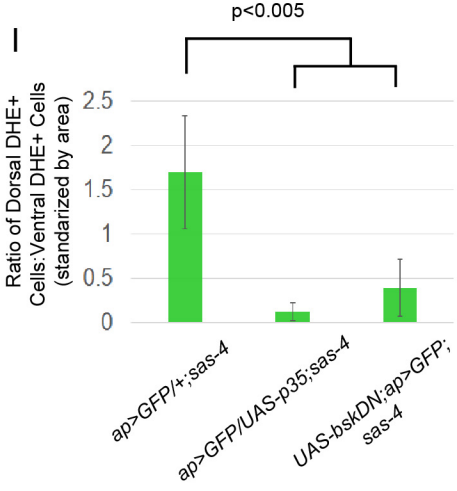
I
p<0.005
Ratio of Dorsal DHE+ Cells:Ventral DHE+ Cells (standarized by area)
2.5
2
1.5
1
0.5
0
ap>GFP/+;sas-4
ap>GFP/UAS-p35;sas-4
UAS-bskDN;ap>GFP; sas-4

Figure 6

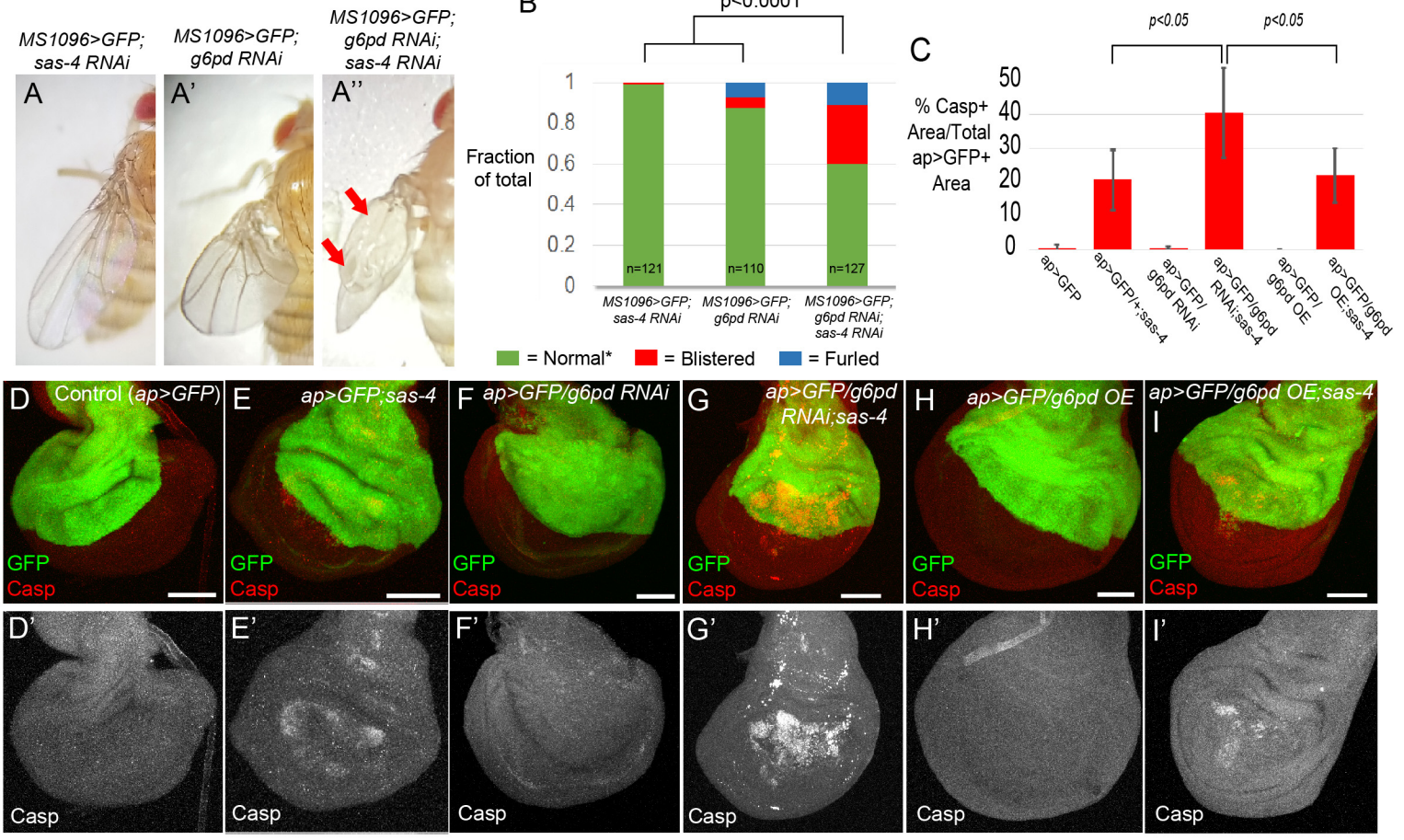
MS1096>GFP; sas-4 RNAi
MS1096>GFP; g6pd RNAi
MS1096>GFP; g6pd RNAi; sas-4 RNAi
A
A'
A''
B
p<0.0001
Fraction of total
1
0.8
0.6
0.4
0.2
0
n=121
n=110
n=127
MS1096>GFP; sas-4 RNAi
MS1096>GFP; g6pd RNAi
MS1096>GFP; g6pd RNAi; sas-4 RNAi
= Normal*
= Blistered
= Furled
C
p<0.05
p<0.05
% Casp+ Area/Total ap>GFP+ Area
50
40
30
20
10
0
ap>GFP
ap>GFP/+;sas-4
ap>GFP/ g6pd RNAi
ap>GFP/g6pd RNAi;sas-4
ap>GFP/ g6pd OE
ap>GFP/g6pd OE;sas-4
D
Control (ap>GFP)
E
ap>GFP;sas-4
F
ap>GFP/g6pd RNAi
G
ap>GFP/g6pd RNAi;sas-4
H
ap>GFP/g6pd OE
I
ap>GFP/g6pd OE;sas-4
GFP
Casp
D'
E'
F'
G'
H'
I'
Casp

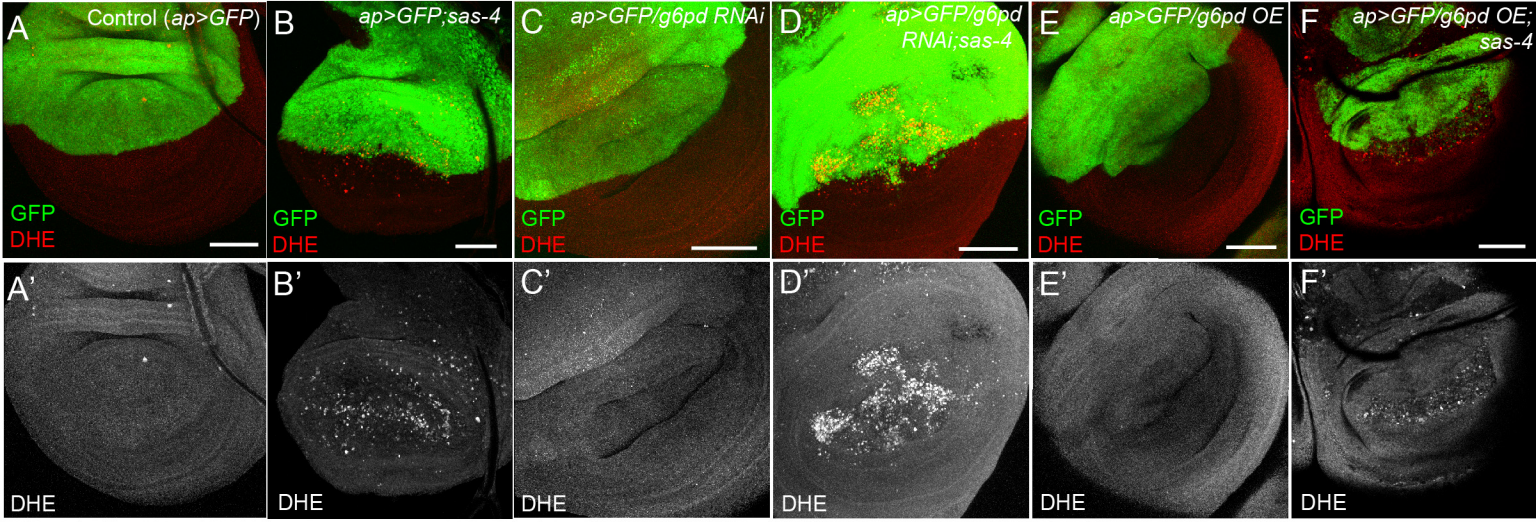

G

Ratio of Dorsal DHE+ Cells: Ventral DHE+ Cells (standarized by area)

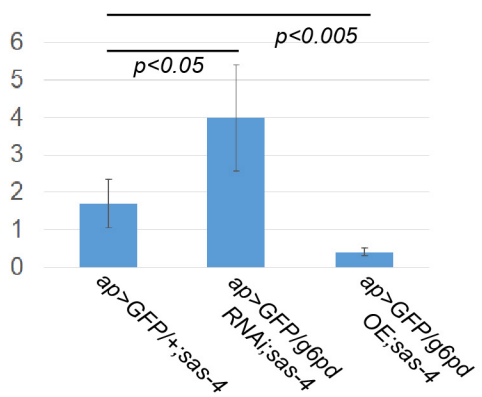

H

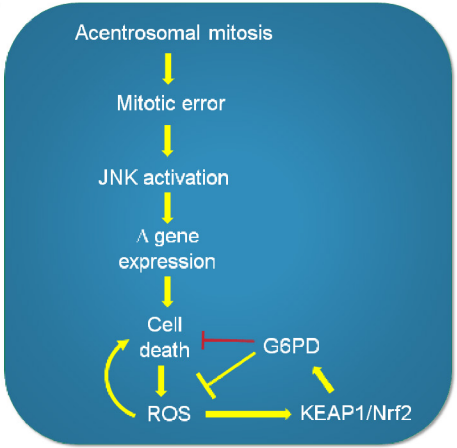

Figure 7

Suppl Figure 1

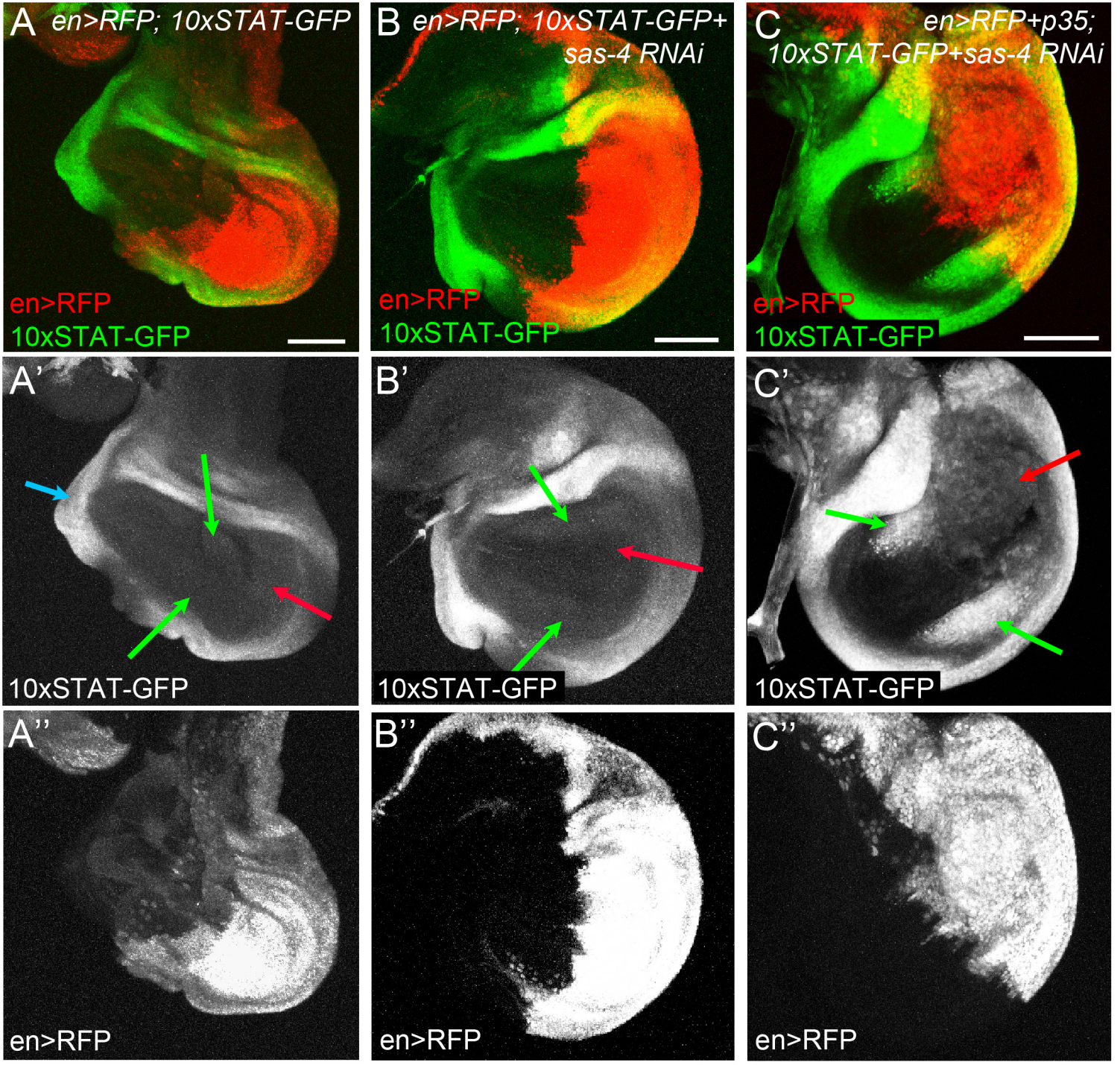

Table 1. GO Terms enriched in genes higher in both *sas-4* and *asl*

Biological Process	**p-value**
Glutathione Metabolic Process	3.90E-04
Imaginal Disc-derived Male Genitalia Morphogenesis	1.20E-03
Cell Adhesion	1.60E-03
Immune Response	5.80E-03
Oxidation-reduction Process	9.20E-03

Molecular Function	**p-value**
Glutathione Peroxidase Activity	8.45E-05
Signaling Pattern Recognition Receptor Activity	3.30E-03

Table 2: Genes with known or putative roles in the oxidative stress response

Gene	Protein Name/Function	Reference
Zw (G6PD)	Zwischenferment. Glucose-6-phosphate dehydrogenase. Rate-limiting enzyme in the pentose phosphate pathway. Reaction generates NADPH, which is used by Glutathione reductase to produce reduced Glutathione (GSH), a potent antioxidant. A Nrf2 target.	Loboda et al, 2016
Glutathione synthase	Second enzyme in synthesis of Glutathione, the key non-enzymatic antioxidant.	Lu, 2013
Traf4	TNF-receptor-associated factor 4. Traf2 regulates oxidative stress with Atg9 through JNK.	Tang et al, 2013
Wwox	WW domain containing oxidoreductase. Regulates ROS and TNF-induced cell death.	O'Keefe et al, 2015
Aox (CG18522)	Aldehyde oxidase 1. Potent generator of superoxides.	Kundu et al, 2012
GstE8	Glutathione-S-transferase E8. Cnc and Paraquat induced. Up in hyperoxia screen.	Greunewald et al, 2009; Misra et al, 2011
GstD3	Glutathione S transferase D3. Cnc and Paraquat induced. Up in hyperoxia screen.	Greunewald et al, 2009; Misra et al, 2011
Men	Malic oxidoreductase. Malic enzyme knockdown modulates reductive stress.	Xie et al., 2013
ImpL3	Lactate dehyrogenase. HIF-1 target gene. Up in hyperoxia screen. Inhibition induces oxidative stress.	Greunewald et al, 2009
Naprt (CG3714)	Nicotinate phosphoribosyltransferase. Rate limiting enzymne in NAD+ syntehsis. NAD+ is a cofactor in redox reastions and helps prevent oxidative stress.	Massudi et al, 2013
AcCoAS	Acetyl Coenzyme A synthase. Mammalian Acss2 promotes acetylation of the stress-responsive Hypoxia Inducible Factor 2α (HIF-2α) subunit by the acetyltransferase/coactivator Creb binding protein (Cbp).	Chen et al, 2017
CG3397	Putative Aldo/keto reductase. Up after hyperoxia oxidative stress.	Greunewald et al, 2009

Table 3: Genes with known or inferred roles in innate immunity or wound healing

Gene	Role	Reference
Immune response or innate immunity target genes		
Dif	NF-KB transcription factor, in Toll pathway.	Buchon et al., 2014
PGRP-LC	Peptidoglycan recognition protein LC. Transmembrane receptor recognizing DAP-type peptidoglycan, a bacetrial cell wall component. Upstream of the Immune Deficiency pathway.	Buchon et al., 2014
PGRP-SA	See above. Other PGRPs are Cnc and Paraquat induced--Involved in the Toll pathway Induced by LPS in S2 cells.	Boutros et al., 2002. Buchon et al., 2014
GNBP2	Gram-negative bacteria binding protein 2.	Buchon et al., 2014
Clect27	C-type lectin. Putative roles in bacterial recognition.	O'Rourke et al., 2006
Spn55B	Serpins function in Toll receptor activation.	Meekins et al., 2017
upd2	Jak/Stat ligand. Required for parasitoid wasp immune repsonse.	Yang and Hultmark, 2016
upd3	Jak/Stat ligand. Required for parasitoid wasp immune repsonse.	Yang and Hultmark, 2016
cv-2	Crossveinless 2, binds BMPs, is an immunity target gene in gut	Buchon et al., 2009
Ipk1	inositol pentakisphosphate 2-kinase. An immunity target gene in gut	Buchon et al., 2009
LamC	Lamin C. An immunity target gene in gut	Buchon et al., 2009
vir-1	virus-induced RNA 1. A JAK-STAT target, induced by viral infection.	Dostert et al., 2005
wun2	Wunen 2. Lipid phosphate phosphatase. An immunity target gene in gut and hemocytes	Boutros et al, 2002; Buchon et al., 2009
Pvf2	Ligand for Pvr pathway. IMD pathway activates Pvf2 and 3 in a JNK dependent way. Induced by LPS in Drosophila S2 cells.	Boutros et al., 2002; Bond and Foley, 2009
myo61f	Required for intestinal brush border integrity and resistance to bacterial pathogens. Induced by LPS	Hegan et al., 2007; Silverman et al., 2003
Jra	Jun transcription factor. Induced by LPS in Drosophila S2 cells.	Boutros et al. 2002
Puc	Puckered. JNK phosphatase. Induced by LPS in Drosophila S2 cells.	Boutros et al. 2002
Ets21c	Ets-domain transcription factor. Induced by LPS in Drosophila S2 cells.	Boutros et al. 2002
RhoL	Rho family GTPase. Induced by LPS in Drosophila S2 cells.	Boutros et al. 2002
Mmp1	Matrix metalloproteinase 1. Induced by LPS in Drosophila S2 cells.	Boutros et al. 2002
Melanization and wound response		
Tg	Transglutaminase. Part of cuticle cross-linking wound response pathway.	Telci and Griffin, 2006
amd	α methyl dopa-resistant. Part of cuticle cross-linking wound response pathway.	Tang, 2009
Ddc	Dopa decarboxylase. Part of cuticle cross-linking wound response pathway.	Tang, 2009
yellow-b	Related to Yellow, which is sufficient for the formation and deposition of melanin.	Ferguson et al., 2010
yellow-c	See above.	Ferguson et al., 2010
Cpr76Bc	Cuticular protein 76Bc. Three other Cprs are known to be wound inducible	Moussian, 2010
mtg	Mind the gap. Chitin binding cuticle protein.	Moussian, 2010
Edg78E	Insect cuticle protein; Chitin-binding.	Moussian, 2010
Mmp1	Matrix metalloproteinase 1. A wound response gene	Lee and Miura, 2014
scb	alpha-integrin. JNK target required for embryonic wound repair.	Campos et al., 2010; Homsy et al.,2005
Jra	Jun-related antigen (=fly Jun). Required for embryonic wound repair.	Campos et al., 2010
Ets21C	Ets family transcription factor. Wound response gene	Patterson et al., 2013

Table 4: Genes related to JNK signaling

Gene	JNK pathway/regulators	Reference
Jra	Jun transcription factor, essential part of JNK pathway. Also a JNK target gene.	Ríos-Barrera and Riesgo-Escovar, 2012
puc	Protein phosphatase that is a feed back negative regulator of JNK. JNK target gene.	Ríos-Barrera and Riesgo-Escovar, 2012
Gadd45	Mammalian relatives are JNK activators. Fly protein genetically interacts with *hep*=Fly JNKK.	Peretz et al., 2007
Pvf1	PDGF- and VEGF-related factor 1. Involved in corpse removal, a role in which it and its receptor Pvr are upstream of JNK.	Ishimaru et al., 2004
Pvf2	PDGF- and VEGF-related factor 2. Activated by IMD pathway in a JNK dependent way and acts with Pvf3 in turn as a feedback negative regulator of JNK signaling.	Bond and Foley, 2009
scaf	Inactive Serine protease. JNK target gene and feedback negative regulator of the JNK pathway.	Rousset et al., 2010
Traf4	TNF-receptor-associated factor 4. Traf2 regulate oxidative stress with Atg9 through the JNK pathway.	Tang et al., 2013; Ríos-Barrera and Riesgo-Escovar, 2012
	JNK Target genes	
ImpL2	Secreted Insulin/IGF Antagonist .	Jasper et al., 2001
Ilp8	Divergent member of the insulin/IGF/relaxin-like family.	La Fortezza et al., 2016
Myo61F	Myo1C. Induction by LPS requires JNK.	Silverman et al., 2003
Nlaz	Neural Lazarillo. A lipocalin involved in metabolic homeostasis.	Hull-Thompson et al., 2009; Kucerova et al., 2016
scb	Integrin alpha-chain.	Homsy et al., 2006
upd2	Unpaired 2. JAK-STAT ligand.	Carlos Pastor-Pareja et al., 2008
upd3	Unpaired 3. JAK-STAT ligand.	Santabarbara-Ruiz, 2015; Carlos Pastor-Pareja et al., 2008
MMP1	Matrix metalloproteinase 1.	Uhlirova and Bohmann, 2006

Table 5. Candidate genes screened for interaction with *sas-4*

RNAi gene target	Stock ID	Crossed to *MS>GFP* alone	Crossed to *MS>GFP;sas-4 RNAi*
Upd2	BDSC 33949	Strongly dysmorphic	Strongly dysmorphic
	BDSC 33988	Not determined	Normal
Ets21C	BDSC 39069	Strongly dysmorphic	Strongly dysmorphic
Castor	VDRC 2929	Normal	Normal
Cnc	VDRC 37674	Normal	Normal
	VDRC 108127	Normal	Normal
	VDRC 101235	Strongly dysmorphic	Strongly dysmorphic
Dif	VDRC 30579	Normal	Normal
	VDRC 100537	Normal	Normal
G6PD	VDRC 101507	All erect, 5% blistered and 7% furled	All erect, 29% blistered and 11% furled
	BDSC 50667	Strongly dysmorphic	Strongly dysmorphic
ImpL3	VDRC 110190	Normal	Normal
	VDRC 31192	Normal	Normal
Jra	VDRC 31595	Normal	Necrotic spots
KEAP1	VDRC 107052	Normal	Normal
	VDRC 330323	Normal	Normal
TRAF4	VDRC 110766	Normal	Normal
MMP1	VDRC 31989	Normal	Normal
WWOX	VDRC 108350	Normal	Normal

Table 6: Known or Suspected Xenobiotic Response Genes

Gene	Role	Reference
Phase 1: Cytochrome p450s		
Cyp18a1	Cytochrome P450-18a1. Part of a superfamily of heme containing microsomal oxidase enzymes that metabolize both xenobiotic compounds for detoxification and endogenous substrates.	Feyereisen, 2005
Cyp6a17	Cytochrome P450-6a17. See above.	Feyereisen, 2005
Cyp6a23	Cytochrome p450-6a23. See above.	Feyereisen, 2005
CG12224	Cytochrome P450 reductase/NADPH:ferrihemoprotein oxidoreductase. Membrane-bound enzyme required for electron transfer to cytochrome P450 in the microsome from NADPH	Pandey and Fluck, 2013
Phase 2: Modify Xenobiotics to increase hydrophilicity		
AcCoAS	Acetyl Coenzyme A synthase. Functions in glycine conjugation of xenobiotics. Cofactor of NATs.	Montooth et al., 2006
St3	Sulfotransferase 3.	James and Ambadapadi, 2013
CG15661	UDP-glucuronosyl/UDP-glucosyltransferase involved in detoxification.	Gruenewald et al., 2009
Aox (CG18522)	Aldehyde oxidase 1. In addition to metabolic roles, catalyzes the oxidation of both cytochrome P450 (CYP450) and monoamine oxidase (MAO) intermediate products.	Yang et al., 2007
GSS	Glutathione synthase	
GstD1	Glutathione-S-transferase D1. JNK and Nrf2 target gene.	Board and Menon, 2013; Misra et al., 2011
GstD3	Glutathione S transferase D3. Nrf2 target.	Misra et al., 2011
GstE3	Glutathione S transferase E3. Nrf2 target.	Misra et al., 2011
GstE5	Glutathione S transferase E5.	Misra et al., 2011
GstE6	Glutathione S transferase E6. Nrf2 target.	Misra et al., 2011
GstE8	Glutathione S transferase E8. Nrf2 target.	Misra et al., 2011
sda	Slamdance or aminopeptidase N. Modifies glutathione-S-conjugate. gamma-glutamyl transpeptidase (GGT), aminopeptidase N (APN) and cysteine-conjugate-β-lyase (CCBL) may comprise a multi-enzyme pathway that acts on xenobiotic-glutathione conjugates.	Hausheer et al., 2011
Men-b	Malic enzyme b. Induced by xenobiotics. May provide NADPH for glutathione reductase and NADPH-cytochrome c reductase.	Oda et al., 1999
Zw (G6PD)	Zwischenferment. Glucose-6-phosphate dehydrogenase. A NRF2 target gene. Provides NADPH to gluthathione reductase.	Loboda et al., 2016
CG10365	Glutathione-specific gamma-glutamylcyclotransferase 1. Similar to mouse Chac1. May destroy glutathione.	Bachhawat and Yadav, 2018
CG18641	Triacylglycerol lipase family. May function in metabolism of 3-phenoxybenzoic acid-containing xenobiotic triacylglycerols.	Lian et al., 2018
CG4267	Triacylglycerol lipase family. See above.	Lian et al., 2018
CG7367	Triacylglycerol lipase family. See above.	Lian et al., 2018
Phase 3: Export Xenobiotics		
l(2)03659	MDR4/MOAT-B. ABC transporter-like.	Hoffman and Kroemer, 2004